Sectoral Uncertainty

by Efrem Castelnuovo,[1] Kerem Tuzcuoglu[2] and Luis Uzeda[3]

[1]University of Padova, CESifo and Centre for Applied Macroeconomic Analysis
efrem.castelnuovo@unipd.it

[2]Financial Stability Department
Bank of Canada
ktuzcuoglu@bank-banque-canada.ca

[3]Canadian Economic Analysis Department
Bank of Canada
luzedagarcia@bank-banque-canada.ca

Acknowledgements

Abstract

We propose a new empirical framework that jointly decomposes the conditional variance of economic time series into a common and a sector-specific uncertainty component. We apply our framework to a large dataset of disaggregated industrial production series for the US economy. Our results indicate that common uncertainty and uncertainty linked to non-durable goods both recorded their pre-pandemic global peaks during the 1973-75 recession. In contrast, durable goods uncertainty recorded its pre-pandemic peak during the global financial crisis of 2008-09. Vector autoregression exercises identify unexpected changes in durable goods uncertainty as drivers of downturns that are both economically and statistically significant, while unexpected hikes in non-durable goods uncertainty are expansionary. Our findings suggest that: (i) uncertainty is heterogeneous at a sectoral level; and (ii) durable goods uncertainty may drive some business cycle effects typically attributed to aggregate uncertainty.

Topics: Business fluctuations and cycles; Econometric and statistical methods; Monetary policy and uncertainty
JEL codes: E32, E44, C51, C55

Résumé

Nous proposons un nouveau cadre empirique qui permet de décomposer simultanément la variance conditionnelle des séries chronologiques de données économiques en deux facteurs : l'incertitude agrégée et l'incertitude sectorielle. Nous appliquons notre cadre à un vaste ensemble de données désagrégées relatives à la production industrielle aux États-Unis. Nos résultats indiquent qu'avant la pandémie, l'incertitude agrégée et l'incertitude liée aux biens non durables ont toutes deux atteint leur sommet durant la récession de 1973-1975. L'incertitude liée aux biens durables a quant à elle culminé pendant la crise financière mondiale de 2008-2009. Des exercices d'autorégression vectorielle permettent d'établir que les variations imprévues de l'incertitude liée aux biens durables sont des facteurs de ralentissement économiquement et statistiquement significatifs, tandis que les hausses inattendues de l'incertitude liée aux biens non durables ont une action expansionniste. Nos résultats donnent à penser que 1) l'incertitude est hétérogène au niveau sectoriel, et 2) l'incertitude liée aux biens durables peut être à l'origine de certains effets du cycle économique qui sont habituellement attribués à l'incertitude agrégée.

Sujets : Cycles et fluctuations économique; Méthodes économétriques et statistiques; Incertitude et politique monétaire
Codes JEL : E32, E44, C51, C55

1 Introduction

Recessions are typically associated with bouts of uncertainty, a stylized fact that has generated considerable research on the role of uncertainty as a driver of the business cycle.[1] More recently, policy institutions such as the International Monetary Fund have raised the importance of implementing sectoral policies to combat the recessionary effects of uncertainty.[2] While such policies have been advocated at the sectoral level, sectoral uncertainty itself remains a theme that has been little explored to date. This may in part be attributed to the technical challenges a researcher has to face to discern what portion of broader (aggregate) uncertainty reflects common (or across-sector) and sectoral (or sector-specific) components. Conceptually, such a task entails (i) the estimation of uncertainty at different layers of economic data; and (ii) the modeling of a reasonably large dataset to pin down all the implications that different dimensions of the economic system may have on uncertainty.

To address points (i) and (ii), this paper proposes a new dynamic factor model that allows for the joint estimation of common and sectoral uncertainty within a data-rich environment. Our strategy is based on a hierarchical factor setting in the spirit of, e.g., Kose et al. (2003), Del Negro and Otrok (2007), Moench et al. (2013), and Gorodnichenko and Ng (2017) that accommodates the different degrees of volatility pervasiveness in economic data. We define uncertainty as the conditional volatility of the unpredictable components of economic indicators. In particular, we parameterize *common* uncertainty as a dynamic factor that is common to the time-varying volatility of *all* variables in a large system. In contrast, *sectoral* uncertainty is modeled as a dynamic factor that is common to the time-varying volatility of a *subset* of variables corresponding to a particular sector. As a result, our methodology breaks down the (conditional) variance of each time series in our setting into two components, a common and sectoral one.

---

[1]Theoretical frameworks formalizing channels that capture the effects of uncertainty shocks on real activity have been proposed by, among others, Bloom (2009), Fernández-Villaverde et al. (2011), Fernández-Villaverde et al. (2015), Leduc and Liu (2016), Basu and Bundick (2017), Bloom et al. (2018), Bianchi et al. (2021), and Born and Pfeifer (2021). Empirical investigations identifying uncertainty as a driver of the business cycles include Caggiano et al. (2014), Jurado et al. (2015), Baker et al. (2016), Caldara et al. (2016), Angelini et al. (2019), Carriero et al. (2016, 2018), Ludvigson et al. (2021), and Coibion et al. (2021). For surveys, see Bloom (2014), Fernández-Villaverde and Guerron-Quintana (2020), and Cascaldi-Garcia et al. (2021).

[2]See, e.g., https://blogs.imf.org/2020/11/19/continued-strong-policy-action-to-combat-uncertainty/.

We apply our new empirical framework to a rich dataset of U.S. industrial production that comprises 185 industry-level production series grouped into two sectors, namely durable and non-durable goods over a sample period from 1972Q1 to 2019Q4.[3] In accordance with conventional wisdom, we document common uncertainty to be countercyclical, display sharp increases during recessions, and feature a positive correlation with popular uncertainty measures such as those of Jurado et al. (2015), Baker et al. (2016), and Ludvigson et al. (2021). Our sectoral uncertainty measures, however, are found to behave heterogeneously. Uncertainty in the nondurable goods sector displays its global peak during the 1973–75 recession, a feature shared with our common uncertainty factor. In contrast, uncertainty in the durable goods sector peaks during the Great Recession of 2008–09, an episode in recent U.S. history clearly characterized by a massive increase in uncertainty (Blanchard, 2009). Furthermore, similar to common uncertainty, we find durables uncertainty to be more tightly linked to a variety of business cycle indicators.

The last part of the paper carries out a VAR analysis that involves a battery of standard macroeconomic indicators (similar to those modeled by Bloom (2009), Fernández-Villaverde et al. (2015), Jurado et al. (2015), Basu and Bundick (2017), and Born and Pfeifer (2021)) and our novel measures of common and sector-specific uncertainty. We document unexpected hikes in uncertainty to generate different responses of real activity depending on the type of uncertainty one considers. In particular, we find three distinct patterns. First, unexpected changes in *common* uncertainty trigger a "drop-rebound-overshoot" dynamic response to real activity in line with the one documented by Bloom (2009).[4] Second, shocks to *durables* uncertainty generate an inverse hump-shaped (or contractionary) response to real activity. Such a result connects our analysis with the literature on the "wait-and-see" (or "real options") behavior of firms and consumers due to non-convex adjustment

---

[3]Given the set of unique circumstances that characterize the COVID-19 pandemic period, extending our analysis to address post-2019Q4 developments arguably warrants a separate study to focus exclusively on uncertainty (common and sectoral) within this period. That said, we stress that our framework exhibits features, such as stochastic volatility and outlier adjustment, that are desirable to model the extreme time-series values witnessed during the COVID-19 pandemic. Also, while we apply our methodology to disaggregated U.S. industrial production data (as, e.g., Foerster et al. (2011) and Garin et al. (2018)), our framework lends itself to a variety of applications in macroeconomics and finance where separating common and sector-specific volatility is important.

[4]Bloom (2009) employs Hodrick-Prescott filtered data in his VAR. Caggiano et al. (2022) show that Bloom's (2009) results are also robust to using unfiltered data.

costs, typically associated with durable goods, as in Bloom (2009) and Bloom et al. (2018). Third, and against conventional wisdom, shocks to *nondurable* goods uncertainty are found to generate an expansionary response in production and employment. Taken together, our results suggest that the countercyclicality of uncertainty, as is usually documented, may in fact be due to a specific subset of goods in the economy, namely durables, rather than the manifestation of a broader phenomenon. Consequently, a complete account of the business cycle effects of uncertainty seems to call for the modeling of sectoral heterogeneities.

We also conduct the above-described VAR analysis on a shorter sample that begins in 1984, which is often referred to as the beginning of the Great Moderation period. Such an exercise reveals the effects of sectoral uncertainty on real activity to be even stronger when compared to results from a sample that also encompasses the 1970s. This last finding, albeit related to second-moment sectoral shocks, matches the timing identified by Foerster et al. (2011), Atalay (2017), and Garin et al. (2018), who document the increased role of first-moment sectoral shocks for the determination of the U.S. business cycle since the mid-1980s. Our VAR results also echo the findings put forth by Horvath (1998, 2000), Conley and Dupor (2003), Acemoglu et al. (2012), Acemoglu et al. (2017), and Baqaee and Farhi (2019), who assert that sectoral shocks can lead to aggregate fluctuations due to network effects, input-output linkages between sectors, nonlinearities, and the presence of large and crucial sectors.

Our paper joins recent research that has also taken a sectoral view on uncertainty. Choi and Loungani (2015) employ stock market data to construct both an aggregate measure of time-series volatility in stock returns and a sectoral measure of cross-industry uncertainty in stock returns. They find sectoral uncertainty to have a different impact on unemployment than common uncertainty. Segal (2019) measures sectoral uncertainty as the shocks to the volatility of sectoral total factor productivity. Akin to our study, the author also provides evidence on the heterogeneous effects of sectoral uncertainty on economic aggregates. Specifically, uncertainty originating in the consumption sector has contractionary effects on macroeconomic growth rates, while investment-related uncertainty has expansionary economic effects. Ma and Samaniego (2019) measure uncertainty as the median absolute forecast errors drawn from a large firm-level dataset. In their setting, median absolute

forecast errors obtained from the full dataset are called common uncertainty, while those obtained from a selected subset of industries are interpreted as sectoral uncertainty.

We differ from these three studies in two key dimensions. First, and to the best of our knowledge, we are the first study to estimate common and sectoral uncertainty *jointly*. Hence, by explicitly parameterizing sectoral uncertainty as a net-of-common component, our setting provides an avenue to sharpen the inference of uncertainty in contexts where defining the latter requires a higher level of granularity. Put differently, our approach reduces the likelihood of confounding common and sectoral uncertainty dynamics, which is a risk one runs when estimating each measure independently (as in Ma and Samaniego (2019)), or sequentially via two-step procedures (as in Choi and Loungani (2015) and Segal (2019)).[5] Second, unlike previous studies, our take on sectoral uncertainty focuses on the goods sector, which is traditionally a sector that exhibits salient dynamics during recessions and downturns (see, e.g, Wynne and Balke (1993) and Kehoe et al. (2018)).

Our paper also adds to recent investigations that combine factor and stochastic volatility methods to deal with uncertainty measurement, such as Carriero et al. (2016, 2018), Jo and Sekkel (2019), and Mumtaz and Musso (2019). In this regard, our contribution is twofold. First, we extend the parametrization for common stochastic volatility models proposed in Carriero et al. (2016, 2018) by combining hierarchical-factor and outlier-adjustment methods that allow for a more flexible representation of second moments in our model. Second, to carry out estimation, we develop an efficient Markov Chain Monte Carlo (MCMC) algorithm that relies on precision sampling methods, as in, e.g., Chan and Jeliazkov (2009). As pointed out in McCausland et al. (2011), precision-based methods typically reduce computational complexity and expedite estimation relative to Kalman filter-based approaches, which are used for state-space inference more broadly.

The remainder of this paper proceeds as follows. Section 2 introduces our empirical framework. Section 3 discusses the estimation of our proposed model. Empirical results are given in Section 4. Section 5 concludes. An Online Appendix contains further details on the dataset, estimation technique, and robustness checks.

---

[5]Regarding two-step methods, while certainly a convenient strategy, they are prone to be affected by the generated regressors problem. Such a problem, as pointed out by Pagan (1984) and Kim and Kim (2011) (also in the context of estimating unobservable series), could ultimately lead to invalid inferences due to potential cumulative measurement errors from previous estimation steps.

2 A Hierarchical Common Stochastic Volatility Model

This section describes our novel empirical framework designed to measure uncertainty in the goods sector at different levels of aggregation. The first issue at hand is how to interpret uncertainty. A common and intuitive way to do so is to treat uncertainty as the volatility of the unpredictable component embedded in a dataset of interest. Such a characterization can be parameterized in the context of a linear regression setting, that is:

$$y_t = X_t \boldsymbol{\beta} + u_t, \tag{1}$$

where the conditional expectation $\mathbb{E}_t(y_t) = X_t \boldsymbol{\beta}$ provides an optimal prediction (in a mean squared error sense) for the $N \times 1$ vector y_t containing a set of economic time-series with observations going from 1 to T, where N identifies the number of industries in our dataset, and T the time-series dimension. Therefore, unpredictability (and, consequently, uncertainty) is associated with the error term u_t.

2.1 Factor-Based Controls

To ensure u_t is unpredictable (or approximately so), it is convenient to define X_t in a manner that extracts as much predictable content as possible from y_t while not overfitting the expression in Equation (1). In our exercise, y_t accounts for 185 (standardized) production growth series at the quarterly frequency from 1972Q1 until 2019Q4. These series are obtained from disaggregated IP data that cover a cross-section of industries in both the durable goods and nondurable goods sectors.[6] A detailed description of the data is provided in Section A3 of the Online Appendix.

Given the large dimension of y_t, adopting a more traditional framework such as a VAR to model X_t would represent a less tractable avenue computationally. Consequently, we

---

[6]Our definition of a sector is based on the North American Industry Classification System (NAICS) where the first two digits in the NAICS structure designate the sector to which an industry belongs. Also, we opt to work with quarterly data since monthly disaggregated IP series are substantially "noisier," and as pointed out by Miron and Zeldes (1989), possibly affected by significant measurement errors in the earlier part of the sample. At the quarterly frequency such errors may, in principle, become less consequential as monthly data is averaged over the quarter. Moreover, quarterly data is a conventional frequency for business cycle-related analysis.

follow studies such as Stock and Watson (2016) and McCracken and Ng (2016) that propose factor-based controls to construct X_t in data-rich environments. Specifically, we organize covariates in X_t into two types of factors, namely factors that capture economic conditions more broadly and factors that capture IP-specific dynamics.

For the first category, we follow McCracken and Ng (2016) and use principal-component techniques to extract common factors from a large cross-section of U.S. economic indicators. These indicators span a wide range of variables within broad categories (e.g., production, labor market, prices, financial markets), which we acquire from the Federal Reserve Economic Macroeconomic Database (FRED-MD hereafter).[7] The testing procedure of Bai and Ng (2002) is then employed to select the optimal number of factors (seven in our application). These factors are then integrated into X_t as "observable" measures. Given the large cross-section of data used to extract the principal components, the generated regressors problem that is commonly associated with treating principal components as actual data becomes less of an issue in the context of our exercise (see Bai and Ng (2008)).

Regarding the IP-specific factors, we treat them as latent factors that are estimated jointly with the other states and parameters in our model (estimation details are discussed in Section 3). To determine the number of IP-specific factors, we apply once again the testing procedure of Bai and Ng (2002), except now the method is applied to the 185 IP growth series in y_t. Since we model these latent factors as a VAR process, we check both the static and dynamic versions of the test statistic proposed by Bai and Ng (2002). We also employ a robust test statistic proposed by Alessi et al. (2010). All these criteria point to four IP-specific factors. Below we summarize how X_t is structured:

$$
\texttt{Controls:} \begin{cases} X_t = [I_N \otimes z_t' \quad I_N \otimes f_t'], \\[2mm] z_t = (z_{1,t}, \cdots, z_{7,t})' \quad - \text{McCracken and Ng (2016) factors}, \\[2mm] f_t = (f_{1,t}, \cdots, f_{4,t})' \quad - \text{IP-specific factors}, \\[2mm] f_t = \Phi_f f_{t-1} + \eta_{f,t} \quad \eta_{f,t} \sim \mathcal{N}\left(0, \texttt{diag}\left(\sigma_{f_1}^2, \cdots, \sigma_{f_4}^2\right)\right), \end{cases} \tag{2}
$$

where I_N and $\otimes$ denote an N-dimensional identity matrix and the Kronecker product,

---

[7]Details on the FRED-MD database can be found in Section A3 of the Online Appendix and at the Federal Reserve Bank of St. Louis website.

respectively. The seven factors from the FRED-MD database and the four IP-specific factors are collected by z_t and f_t, respectively. The latter, as shown in the last expression in (2), is modeled as a (four-variable) first-order VAR with homoskedastic innovations. The constant-variance assumption is relaxed in Section 4.5, where we allow for stochastic volatility to model the conditional volatility of $\eta_{f,t}$ in the context of robustness checks applied to our baseline framework. We note, however, that our key findings are largely unchanged when stochastic volatility is introduced to model second-moment dynamics for f_t.

2.2   Identifying Sectoral Uncertainty

The notion of uncertainty derived from (1) has represented the building block for various studies, as in, *inter alia*, Jurado et al. (2015), Carriero et al. (2016), Jo and Sekkel (2019), and Clark et al. (2020). We thus build on these papers to adopt a hierarchical structure that characterizes uncertainty across the entire goods sector as well as within its sectoral subcomponents, namely the durable and nondurable sectors. To this end, we first cast u_t as:

$$u_t = \Psi_t^{\frac{1}{2}} \Sigma_t^{\frac{1}{2}} e_t, \quad s.t.\ e_t \sim \mathcal{N}\left(0,\ I_N\right), \tag{3}$$

$$\Sigma_t^{\frac{1}{2}} = \mathtt{diag}\left(\exp(h_{1,t}/2), \cdots, \exp(h_{N,t}/2)\right), \tag{4}$$

$$\Psi_t^{\frac{1}{2}} = \mathtt{diag}\left(\psi_{1,t}^{\frac{1}{2}}, \cdots, \psi_{N,t}^{\frac{1}{2}}\right). \tag{5}$$

Equations (3)–(5) indicate that the evolution of the volatility of u_t is expressed in terms of two time-varying components, which we define as follows: (i) $\Sigma_t^{\frac{1}{2}}$ captures volatility changes that are associated with uncertainty dynamics across and within the subcomponents of the goods sector; such dynamics are modeled in the tradition of stochastic volatility models (see, e.g., Kim et al. (1998) and Omori et al. (2007)) and absorbed by the state variables (or log-volatilities) $h_{i,t}$ for $i = 1, ..., N$; and (ii) $\Psi_t^{\frac{1}{2}}$ captures changes in volatility that are idiosyncratic to each industry, i.e., to each element in u_t. We now turn to discuss the modeling of each of these time-varying volatility components in greater detail.

Our goal is to formulate a framework that distinguishes between uncertainty that is

common across and within the durables and nondurables sectors. Also, in keeping with uncertainty-based theories of the business cycle, which typically presuppose common variation in uncertainty across a large number of series, we want our framework to generate uncertainty measures that reflect pervasiveness. As a result, we adopt a factor-based approach that extracts comovement in second moments at different levels of aggregation. In particular, we build upon the work on common stochastic volatility models by Carriero et al. (2016, 2018) to parameterize the vector of log-volatilities $h_t = (h_{1,t}, \cdots, h_{N,t})'$ in (4) as follows:

$$h_t = \Lambda_c v_{c,t} + \Lambda_s v_{s,t}. \tag{6}$$

Equation (6) implies that uncertainty is decomposed into two parts: (i) a factor $v_{c,t}$ that captures the *common* component of uncertainty across all industries in the goods sector; and (ii) a vector $v_{s,t} = (v_{d,t} \ v_{nd,t})'$, where each element denotes a factor that captures the *sector-specific* component of uncertainty in the durables ($v_{d,t}$) and nondurables ($v_{nd,t}$) sectors. To sum up, $v_{c,t}$ and $v_{s,t}$ collect our estimates (in log-volatility form) of across- and within-sector uncertainty, respectively.[8]

To identify uncertainty at such different levels of aggregation, we parameterize the factor-loading matrices as follows:

$$\Lambda_c = \begin{bmatrix} \lambda_{c,1} \\ \lambda_{c,2} \\ \vdots \\ \vdots \\ \lambda_{c,N} \end{bmatrix} \quad \text{and} \quad \Lambda_s = \begin{bmatrix} \lambda_{d,1} & 0 \\ \vdots & \vdots \\ \lambda_{d,S_d} & 0 \\ 0 & \lambda_{nd,1} \\ \vdots & \vdots \\ 0 & \lambda_{nd,S_{nd}} \end{bmatrix}, \tag{7}$$

where S_d and S_{nd} denote the number of industries in the durable and nondurable sectors, respectively (i.e., $S_d + S_{nd} = N$). The characterization above implies that common uncertainty loads on all N industries in our dataset, while durable- and nondurable-specific

---

[8]Once we obtain volatility estimates in the logarithmic scale, we convert results to conditional variances by computing $\exp(v_{j,t})$ for $j = c, \ d, \ nd$.

uncertainty loads only on the industries corresponding to these two sectors. Also, as is standard in factor models, $\lambda_{c,1}$, $\lambda_{d,1}$, and $\lambda_{nd,1}$ are normalized to one in order to separately identify $v_{c,t}$ and $v_{s,t}$ from Λ_c and Λ_s, respectively. In particular, our normalization strategy for the sectoral uncertainty factors follows from multilevel-factor studies such as Moench et al. (2013).[9] In practice, the parameterization given by (6) and (7) implies that the level of overall uncertainty for each industry (i.e., $\exp(h_{i,t}/2)$ for $i = 1, ..., N$) is governed by an economy-wide and a sector-specific component. This nuanced representation is useful as it will allow us to examine potentially heterogeneous effects of goods-related uncertainty on economic activity, a theme we return to in Section 4.3.

Our framework also accommodates the possibility that uncertainty may "spillover" across and within sectors. Such interdependencies are formulated by letting the common and sector-specific factors described above evolve as a VAR process of order one, i.e.:

$$\underbrace{\begin{bmatrix} v_{c,t} \\ v_{d,t} \\ v_{nd,t} \end{bmatrix}}_{v_t} = \Phi_v \underbrace{\begin{bmatrix} v_{c,t-1} \\ v_{d,t-1} \\ v_{nd,t-1} \end{bmatrix}}_{v_{t-1}} + \underbrace{\begin{bmatrix} \eta_{c,t} \\ \eta_{d,t} \\ \eta_{nd,t} \end{bmatrix}}_{\eta_{v,t}}, \tag{8}$$

where we assume the errors in the vector η_t are normally distributed as well as mutually and serially orthogonal to each other.[10]

Note that the parameterization in (6) builds on the work of Carriero et al. (2016, 2018), but provides a key extension to them. Specifically, Carriero et al. (2016), in the context of a VAR model, allow for a single common factor driving the conditional volatility of all variables in the system, but do not explore the idea of group-specific common volatility. In contrast, Carriero et al. (2018) explore the latter idea to distinguish between macroeconomic and financial uncertainty, but do not account for a common factor between these two

---

[9] The block exogeneity restrictions imposed on the loadings provide an intuitive way to identify the latent factors in our model. We acknowledge, however, the existence of other data-driven approaches to interpret factors, such as checking the correlations between the factors and series (Ludvigson and Ng, 2009) and applying shrinkage methods to the loadings (Hacioglu Hoke and Tuzcuoglu, 2016).

[10] We assume the errors in η_t are mutually orthogonal to be consistent with our definition that the common uncertainty factor is the term that captures the (uncertainty-related) contemporaneous correlation amongst the durables and nondurables sectors. Consequently, the remaining errors driving the (sector-specific) factors in (8) should be orthogonal to the rest of the system.

groups. In other words, in light of (6), the proposal put forth by Carriero et al. (2016) can be interpreted as imposing the restriction $\Lambda_s = 0$, while Carriero et al. (2018) impose $\Lambda_c = 0$. Our framework nests both cases. We view the joint modeling of across- and within-group comovement as crucial to avoid potential distortions in the measurement of common and sector-specific uncertainty.

2.3   Idiosyncratic Volatility

Given the large cross-section of industries ($N = 185$) that make up the durables and nondurables sectors in our dataset, it is likely that the production from these industries may exhibit substantial variability amongst themselves and over time. This suggests that the volatility associated with the residual term u_t might be, in part, idiosyncratic rather than pervasive. As show in (3), we accommodate such a possibility by setting $u_t = \Psi_t^{\frac{1}{2}}\Sigma_t^{\frac{1}{2}}e_t$, where industry-specific volatility changes are captured by each element in the scale matrix $\Psi_t^{\frac{1}{2}} = \mathtt{diag}\left(\psi_{1,t}^{\frac{1}{2}}, \cdots, \psi_{N,t}^{\frac{1}{2}}\right)$. More precisely, we define:

$$\psi_{i,t} \overset{i.i.d.}{\sim} \mathcal{IG}\left(\frac{\nu_\psi}{2}, \frac{\nu_\psi}{2}\right) \text{ for } i = 1, \cdots, N \text{ and } t = 1, \cdots, T, \tag{9}$$

where $\mathcal{IG}$ denotes the inverse-gamma distribution. Such a choice of probability distribution and its parameterization follows directly from, e.g., Jacquier et al. (2004) and Chib et al. (2006), where the authors adopt a similar decomposition of the error covariance matrix to the one in (3). Notably, in addition to absorbing series-specific volatility, $\psi_{i,t}$ turns the distribution of the composite error term $u_t = \Psi_t^{\frac{1}{2}}\Sigma_t^{\frac{1}{2}}e_t$, marginalized over $\Psi_t^{\frac{1}{2}}$, into a random variable that follows a Student-t distribution with ν_ψ degrees of freedom.[11] As a result, since the t-distribution is a fat-tailed distribution, the introduction of Ψ_t provides our framework with a form of outlier adjustment. This is empirically useful as it allows our framework to accommodate a distinction between what constitutes sizeable series-specific volatility and uncertainty dynamics. The latter, as previously argued, tend to viewed as a

---

[11]See, e.g., Koop et al. (2007), chapter 15, for a formal presentation of the above-mentioned result. To allow the error distribution to have (*a priori*) heavier tails than those of the Gaussian distribution, we set the degree of freedom parameter ν_ψ at six.

more widespread phenomenon.[12]

An alternative way to model idiosyncratic volatility is the one proposed by Carriero et al. (2018), who introduce a series-specific error term into the log-volatility state equation (6) to model 18 macroeconomic time-series. Unfortunately, this approach is unfeasible in our framework, because this would require us to augment our posterior simulation algorithm to estimate as many log-volatility states as there are variables in y_t, i.e., 185. Estimating such a large number of log-volatility states makes computation virtually prohibitive.

3   Estimation

Our framework constitutes a nonlinear state space model. As is common in such instances, we conduct estimation using Bayesian methods. In particular, we propose an estimation algorithm that is fully based on Gibbs sampling steps. Briefly, we develop an MCMC algorithm, whereby we retain 50,000 draws from the 60,000 runs of our MCMC sampler. The first 10,000 burn-in draws are discarded. Results for the mixing efficiency of the MCMC chain are presented in Section A1 of the Online Appendix. We note here that the mixing of our algorithm is quite good.

To facilitate the description of our estimation strategy, we make use of additional notation. Specifically, we define $\boldsymbol{\theta}$ and $\mathcal{Z}$ as the sets containing, respectively, the parameters and latent states in our model, while $\boldsymbol{\theta}_{-\mathbf{j}}$ and $\mathcal{Z}_{-\mathbf{j}}$ will be used as short notation when these sets contain all their elements except for j. Also, hereafter we make use of the following stacked representation for y_t, i.e., $\mathbf{y} = (y_1, \cdots, y_T)'$. At a high level, our estimation framework consists of two main blocks, namely parameter sampling and state simulation. Below we discuss these two blocks in turn.

3.1   Parameter Sampling

We begin by setting $\boldsymbol{\theta} = \{\tilde{\boldsymbol{\beta}}_z, \ \tilde{\boldsymbol{\beta}}_f, \ \tilde{\boldsymbol{\lambda}}_c, \ \tilde{\boldsymbol{\lambda}}_d, \ \tilde{\boldsymbol{\lambda}}_{nd}, \ \boldsymbol{\phi}_f, \ \boldsymbol{\phi}_v, \ \boldsymbol{\sigma}_f^2, \ \boldsymbol{\sigma}_v^2\}$, where the first five elements in $\boldsymbol{\theta}$ denote vectors collecting the loading coefficients in (1) and (6). To be clear,

---

[12]Following the COVID-19 pandemic, stochastic volatility models with outlier adjustment have witnessed a renewed interest. See, e.g., Antolín-Díaz et al. (2020), Carriero et al. (2020); Marcellino et al. (2021)), and Lenza and Primiceri (2021) for recent applications.

$\tilde{\boldsymbol{\beta}}_z$ collects the coefficients that are associated with the FRED-MD factors (z_t), which—as discussed in Section 2.1—are treated as observables. The vector $\tilde{\boldsymbol{\beta}}_f$ collects the coefficients that load on the IP-specific factors (f_t), which are treated as latent variables. As a result, $\tilde{\boldsymbol{\beta}}_f$ excludes coefficients that are normalized to one since these do not need to be sampled. The same rationale applies to $\tilde{\boldsymbol{\lambda}}_c$, $\tilde{\boldsymbol{\lambda}}_d$, and $\tilde{\boldsymbol{\lambda}}_{nd}$, which collect the loadings associated with the latent common, durables, and nondurables uncertainty factors, respectively. Next, let `vec` stand for the operator that transforms a matrix into a column vector. The terms $\boldsymbol{\phi}_f = \texttt{vec}(\Phi'_f)$ and $\boldsymbol{\phi}_v = \texttt{vec}(\Phi'_v)$ thus denote vectors collecting the coefficients in the VAR-based law of motion for f_t and v_t in (2) and (8), respectively. Lastly, $\boldsymbol{\sigma}^2_f$ and $\boldsymbol{\sigma}^2_v$ denote vectors containing the variances associated with the error terms in the state equations for f_t and v_t, respectively. The parameter-sampling block of our MCMC algorithm can thus be summarized by sequentially drawing from the following distributions:

$$
\texttt{MCMC Steps:} \quad
\begin{cases}
(1)\ p\left(\tilde{\boldsymbol{\beta}}_x | \mathbf{y}, \mathcal{Z}, \boldsymbol{\theta}_{-\tilde{\beta}_x}\right) & \text{for } x = z,\ f, \\[6pt]
(2)\ p\left(\tilde{\boldsymbol{\lambda}}_j | \mathbf{y}, \mathcal{Z}, \boldsymbol{\theta}_{-\tilde{\lambda}_j}\right) & \text{for } j = c,\ d,\ nd, \\[6pt]
(3)\ p\left(\boldsymbol{\phi}_\ell | \mathbf{y}, \mathcal{Z}, \boldsymbol{\theta}_{-\phi_\ell}\right), \\[6pt]
(4)\ p\left(\boldsymbol{\sigma}^2_\ell | \mathbf{y}, \mathcal{Z}, \boldsymbol{\theta}_{-\sigma^2_\ell}\right) & \text{for } \ell = v,\ f.
\end{cases}
\tag{10}
$$

To sample from each of the MCMC steps above, we adopt mutually independent priors. More specifically, for each element in $\tilde{\boldsymbol{\beta}}_x$, $\tilde{\boldsymbol{\lambda}}_j$, and $\boldsymbol{\phi}_\ell$ we elicit a Gaussian prior given by $\mathcal{N}\left(\hat{\mu}_l,\ \hat{\sigma}^2_l\right)$ for $l = \tilde{\beta}_x,\ \tilde{\lambda}_j,\ \phi_\ell$. For the coefficients in $\boldsymbol{\phi}_v$, $\boldsymbol{\phi}_f$, and $\tilde{\boldsymbol{\beta}}_z$ we set $\hat{\mu}_{\tilde{\beta}_z} = \hat{\mu}_{\phi_\ell} = 0$ and $\hat{\sigma}^2_{\tilde{\beta}_z} = \hat{\sigma}^2_{\phi_\ell} = 1$ such that $\ell = v,\ f$. Differently, for the loadings in $\tilde{\boldsymbol{\beta}}_f$, $\tilde{\boldsymbol{\lambda}}_c$, $\tilde{\boldsymbol{\lambda}}_d$, and $\tilde{\boldsymbol{\lambda}}_{nd}$, akin to Carriero et al. (2017), our priors are more tightly parameterized around the normalization condition, i.e., $\hat{\mu}_{\tilde{\beta}_f} = \hat{\mu}_{\tilde{\lambda}_j} = 1$ and $\hat{\sigma}^2_{\tilde{\beta}_f} = \hat{\sigma}^2_{\tilde{\lambda}_j} = 0.01^2$ for $j = c,\ d,\ nd$. For each variance parameter in $\boldsymbol{\sigma}^2_\ell$, we adopt an inverse-gamma prior given by $\mathcal{IG}\left(\nu_\ell,\ S_\ell\right)$ such that $l = v,\ f$. In particular, we set $S_v = 0.2^2(\nu_v - 1)$ and $S_f = (\nu_f - 1)$. The last two expressions imply that $\mathbb{E}\sigma^2_v = 0.2^2$ and $\mathbb{E}\sigma^2_f = 1$, respectively. These imply that we allow, *a priori*, for larger variations in f_t relative to v_t, consistent with our goal to let the former absorb as much predictable content in $\mathbf{y}$ as possible. Such prior beliefs are, however, diffuse

and reflected in the calibration of the shape hyperparameters $\nu_v = \nu_f = \frac{T}{10}$.[13] Notably, the priors discussed above lead to closed-form expressions for all the conditional posterior distributions in (10). These expressions are standard and, for the sake of brevity, are reported in Section A1 of the Online Appendix. Also, our main results carry over to a number of sensitivity checks to the above-described priors. Such checks are discussed in greater detail in Section 4.5.

3.2 State Simulation

Let $\psi_t = (\psi_{1,t}, \cdots \psi_{N,t})'$, while f_t and v_t are defined as in (2) and (8), respectively. We can then group the latent states in our model as $\mathcal{Z} = \{\boldsymbol{\psi}, \mathbf{f}, \mathbf{v}\}$, where $\boldsymbol{\psi} = (\psi_1, \cdots, \psi_T)$, $\mathbf{f} = (f_1, \cdots, f_T)$, and $\mathbf{v} = (v_1, \cdots, v_T)$. State simulation thus entails sampling from the following three distributions:

$$
\text{MCMC Steps:} \begin{cases} (5) \ p\left(\boldsymbol{\psi}|\mathbf{y}, \mathcal{Z}_{-\boldsymbol{\psi}}, \boldsymbol{\theta}\right), \\[2mm] (6) \ p\left(\mathbf{f}|\mathbf{y}, \mathcal{Z}_{-\mathbf{f}}, \boldsymbol{\theta}\right), \\[2mm] (7) \ p\left(\mathbf{v}|\mathbf{y}, \mathcal{Z}_{-\mathbf{v}}, \boldsymbol{\theta}\right). \end{cases} \tag{11}
$$

Step 5 entails sequentially drawing from an inverse-gamma distribution to obtain NT draws for $\psi_{i,t}$. This result follows directly from the inverse-gamma prior in (9). Draws for $\mathbf{f}$ are obtained using the precision sampling methods by Chan and Jeliazkov (2009). The advantage of following this route is that precision methods typically reduce computational complexity and expedite state simulation (McCausland et al., 2011). For brevity, we relegate the expressions for the conditional posterior distributions in Steps 5 and 6 to Section A1 of the Online Appendix. We now discuss how to generate draws for $\mathbf{v}$ from the distribution in Step 7, which is a key feature of our estimation strategy.[14]

---

[13]See, e.g., Kroese and Chan (2014), chapter 11, for details on the parametrization of the inverse-gamma distribution which we adopt.

[14]The initial conditions for f_t and v_t are treated as additional parameters to which we assign a diffuse Gaussian prior centered at zero. We augment our MCMC algorithm to sample such parameters accordingly. The idiosyncratic volatility state ($\psi_{i,t}$) is assumed to be serially uncorrelated and therefore does not require an initial condition.

Joint Sampling of Common and Sector-Specific Uncertainty

Note first that, using the factorization of the error term in (3), the expressions (1), (6), and (8) can be described using the following stack representation:

$$\mathbf{y} = \mathbf{X}\boldsymbol{\beta} + \mathbf{L}_\Psi \mathbf{L}_h \mathbf{e}, \tag{12}$$

$$\mathbf{h} = \boldsymbol{\Lambda}\mathbf{v}, \tag{13}$$

$$\mathbf{L}_{\Phi_v}\mathbf{v} = \widetilde{\mathbf{v}}_0 + \boldsymbol{\eta}_\mathbf{v}, \tag{14}$$

where:

$$\mathbf{X} = \begin{bmatrix} I_N \otimes z_1' & I_N \otimes f_1' \\ \vdots & \vdots \\ I_N \otimes z_T' & I_N \otimes f_T' \end{bmatrix}, \quad \boldsymbol{\beta} = \begin{bmatrix} \boldsymbol{\beta}_z \\ \boldsymbol{\beta}_f \end{bmatrix}, \quad \boldsymbol{\Lambda} = I_T \otimes \begin{bmatrix} \Lambda^c & \Lambda^s \end{bmatrix},$$

$$\mathbf{L}_h = \mathtt{diag}\left(\Sigma_1^{\frac{1}{2}}, \cdots, \Sigma_T^{\frac{1}{2}}\right), \quad \mathbf{L}_\Psi = \mathtt{diag}\left(\Psi_1^{\frac{1}{2}}, \cdots, \Psi_T^{\frac{1}{2}}\right), \quad \mathbf{L}_{\Phi_v} = \begin{bmatrix} I_3 & \mathbf{0} & \cdots & & \mathbf{0} \\ -\Phi_v & I_3 & & & \\ \mathbf{0} & -\Phi_v & \ddots & & \vdots \\ \vdots & & \ddots & & \\ \mathbf{0} & & \cdots & -\Phi_v & I_3 \end{bmatrix}.$$

The vector $\widetilde{\mathbf{v}}_0 = \iota_0 \otimes (\Phi_v v_0)$ collects the initial conditions for the common and sectoral uncertainty measures, where ι_0 denotes a $T \times 1$ vector given by $\iota_0 = (1,\ 0, \cdots, 0)'$.

To estimate $\mathbf{v}$, we combine the auxiliary mixture sampler approach of Omori et al. (2007) with precision sampling techniques. To apply the former, we first recast (12) as $(\mathbf{L}_\Psi)^{-1}(\mathbf{y} - \mathbf{X}\boldsymbol{\beta}) = \mathbf{L}_h \mathbf{e}$, or, more compactly, $\widetilde{\mathbf{y}} = \mathbf{L}_h \mathbf{e}$. Squaring and subsequently taking natural logarithms of each element in both sides of the previous expression yields:

$$\widetilde{\mathbf{y}}^* = \mathbf{h} + \widetilde{\mathbf{e}}^*, \tag{15}$$

where $\widetilde{\mathbf{y}}^* = (\log(\widetilde{y}_1^2), \cdots, \log(\widetilde{y}_T^2))$ and $\widetilde{\mathbf{e}}^* = (\log(e_1^2), \cdots, \log(e_T^2))$.

Next, plugging (13) into the right-hand side of (15) and appending (14) returns:

$$\widetilde{\mathbf{y}}^* = \mathbf{\Lambda}\mathbf{v} + \widetilde{\mathbf{e}}^*, \tag{16}$$

$$\mathbf{L}_{\Phi_v}\mathbf{v} = \widetilde{\mathbf{v}}_0 + \boldsymbol{\eta}_{\mathbf{v}}, \tag{17}$$

which denotes a linear state space form in $\mathbf{v}$. Nevertheless, the squaring and log-transformation applied to the error vector $\mathbf{e}$ implies that each entry in $\widetilde{\mathbf{e}}^*$ now follows a log chi-square distribution with one degree of freedom. To bring (16)–(17) back to a Gaussian (and hence more tractable) form, Omori et al. (2007) suggest approximating the distribution of $\widetilde{\mathbf{e}}^*$ as a ten-component weighted sum (or finite mixture) of Gaussian densities:[15]

$$\widetilde{\mathbf{e}}^* \sim p_1 \mathcal{N}\left(\boldsymbol{\alpha}_1,\ \boldsymbol{\Sigma}_1\right) + \cdots + p_{10}\mathcal{N}\left(\boldsymbol{\alpha}_{10},\ \boldsymbol{\Sigma}_{10}\right). \tag{18}$$

Notably, the values for $\boldsymbol{\alpha}_k$, $\boldsymbol{\Sigma}_k$, and p_k for $k = 1, \cdots, 10$ are predetermined and given in Table 1 of Omori et al. (2007). Therefore, conditional on a particular density in (18), the state space in (16)–(17) can be recast in (conditionally) Gaussian form as:

$$\widetilde{\mathbf{y}}^* = \mathbf{\Lambda}\mathbf{v} + \boldsymbol{\alpha}_k + \widetilde{\mathbf{e}}_k^*, \tag{19}$$

$$\mathbf{L}_{\Phi_v}\mathbf{v} = \widetilde{\mathbf{v}}_0 + \boldsymbol{\eta}_{\mathbf{v}}, \tag{20}$$

$$\begin{bmatrix} \widetilde{\mathbf{e}}_k^* \\ \boldsymbol{\eta} \end{bmatrix} \sim \mathcal{N}\left(\begin{bmatrix} \mathbf{0} \\ \mathbf{0} \end{bmatrix},\ \begin{bmatrix} \boldsymbol{\Sigma}_k & \mathbf{0} \\ \mathbf{0} & \boldsymbol{\Sigma}_{\mathbf{v}} \end{bmatrix} \right), \tag{21}$$

where $\boldsymbol{\Sigma}_{\mathbf{v}} = I_T \otimes \mathtt{diag}(\sigma_{v_c}^2,\ \sigma_{v_d}^2,\ \sigma_{v_{nd}}^2)$. Given the parameterization above, our posterior sampler needs to be augmented to sample a discrete state variable $k_t \in \{1, \cdots, 10\}$ for $t = 1, ..., T$ that serves as the mixture component indicator in (18) and thus determines the values for $\boldsymbol{\alpha}_k$ and $\boldsymbol{\Sigma}_k$ in (19)–(21). More precisely, estimation of $\mathbf{v}$ requires sequentially

---

[15]Their approach extends the seven-component auxiliary mixture sampling from Kim et al. (1998).

sampling from the following two full conditional posterior distributions:[16]

Step 1 $p(\mathbf{k}|\widetilde{\mathbf{y}}^*, \mathcal{Z}, \boldsymbol{\theta})$ $s.t.$ $\mathbf{k} = (k_1, \cdots, k_T)$,

Step 2 $p(\mathbf{v}|\widetilde{\mathbf{y}}^*, \mathcal{Z}_{-\mathbf{v}}, \mathbf{k}, \boldsymbol{\theta})$.

Posterior draws for $\mathbf{k}$ are obtained by independently sampling each element in $\mathbf{k}$ from a multinomial distribution via the inverse transform method as discussed in Kroese and Chan (2014).[17]

Conditional on $\mathbf{k}$ (and the remaining states and parameters), we then combine likelihood- and prior-based information from (19) and (20), respectively, using Bayes rule to obtain the following closed-form expression for $p(\mathbf{v}|\widetilde{\mathbf{y}}^*, \mathcal{Z}_{-\mathbf{v}}, \boldsymbol{\theta})$:

$$\mathbf{v}|\widetilde{\mathbf{y}}^*, \mathcal{Z}_{-\mathbf{v}}, \boldsymbol{\theta} \sim \mathcal{N}\left(\overline{\mathbf{d}}_v, \ \overline{\mathbf{D}}_v\right), \ \text{where} \ \begin{cases} \overline{\mathbf{d}}_v = \overline{\mathbf{D}}_v \left(\boldsymbol{\Lambda}' \boldsymbol{\Sigma}_k^{-1}(\widetilde{\mathbf{y}}^* - \boldsymbol{\alpha}_k) + \mathbf{L}'_{\Phi_v} \boldsymbol{\Sigma}_{\mathbf{v}}^{-1} \widetilde{\mathbf{v}}_0\right), \\ \overline{\mathbf{D}}_v = \left(\boldsymbol{\Lambda}' \boldsymbol{\Sigma}_k^{-1} \boldsymbol{\Lambda} + \mathbf{L}'_{\Phi_v} \boldsymbol{\Sigma}_{\mathbf{v}}^{-1} \mathbf{L}_{\Phi_v}\right)^{-1}. \end{cases} \quad (22)$$

Draws from $\mathcal{N}\left(\overline{\mathbf{d}}_v, \ \overline{\mathbf{D}}_v\right)$ are obtained using the precision sampling techniques as in Chan and Jeliazkov (2009) to construct $\overline{\mathbf{d}}_v$ and $\overline{\mathbf{D}}_v$. Once draws for $\mathbf{v}$ (and for the loadings in $\boldsymbol{\Lambda}_v$) are generated, we plug them into (13) to back out the log-volatilities for the appropriate levels of aggregation.

4   Empirical Results

In this section we present the empirical results obtained from the estimation of the model discussed in Sections 2 and 3. First, we analyze the evolution of common and sectoral uncertainty and discuss how they correlate with other macroeconomic and uncertainty indicators. Second, we conduct a VAR exercise akin to Jurado et al. (2015) to examine the role of uncertainty (both common and sectoral) as drivers of economic activity. In the last

---

[16]The ordering of Steps 1 and 2 shown above is consistent with the discussion in Del Negro and Primiceri (2015) on estimating stochastic volatility models with auxiliary mixture methods.

[17]Further details on how to sample from $p(\mathbf{k}|\widetilde{\mathbf{y}}^*, \mathcal{Z}, \boldsymbol{\theta})$ are provided in Section A1 of the Online Appendix.

part of this section we discuss some robustness checks.

To avoid confusion, it is worth reiterating that we obtain measures of uncertainty from a large cross-section of standardized growth rates for 185 industries allocated evenly across the durable and nondurables sectors in the U.S. economy from 1972Q1 to 2019Q4. Therefore, our common uncertainty measure can be perceived as metric for uncertainty in the goods sector as a whole, while sectoral uncertainty denotes uncertainty that is specific to the durables and nondurables sectors.

4.1 Common Uncertainty

Figure 1 shows the evolution of our estimated common uncertainty factor. In keeping with conventional wisdom (Bloom, 2014), common uncertainty peaks during recessions. In particular, according to our model, (pre-pandemic) uncertainty peaked in the mid-1970s during the first energy crisis of that decade. The second highest peak is associated with the Great Recession of 2008–09. Other distinctive peaks can be seen in the late 1970s and early 1980s, periods respectively characterized by the second energy crisis of the 1970s and restrictive monetary policy—the latter in light of the decade-long period of double-digit inflation that characterized the 1970s. We also document that common uncertainty has become, on average, substantially lower since the mid-1980s. This reinforces the idea put forward by various authors (e.g., Stock and Watson (2002), Sims and Zha (2006), and Galí and Gambetti (2009)) that the Great Moderation is a period predominantly characterized by low overall volatility.

Next, we contrast our estimated measure of common uncertainty against other common measures of broader uncertainty. For this exercise, we adopt the macroeconomic uncertainty indicator of Jurado et al. (2015) (JLN Macro, hereafter), the news data-based economic policy uncertainty index of Baker et al. (2016), the real activity uncertainty index of Ludvigson et al. (2021) (LMN Real, hereafter), and the VIX, used, e.g., by Bloom (2009).

Figure 1: Common Uncertainty
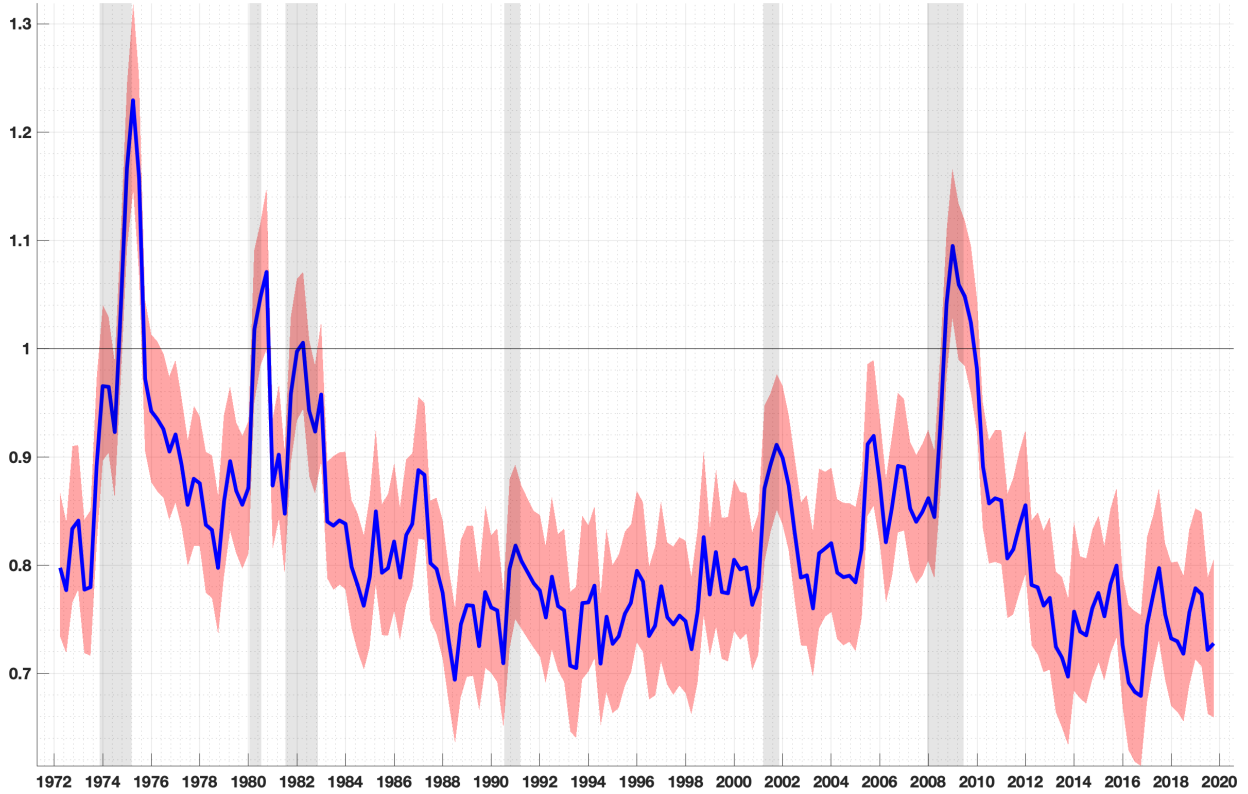
Notes: Common uncertainty is extracted from disaggregated IP data for 185 industries using the modeling approach discussed in Sections 2 and 3. The solid line denotes the posterior median for $\exp(v_{c,t}/2)$. The shaded region denotes the 67% equal-tailed posterior credible interval. The vertical shaded bars correspond to the NBER recession dates.

Figure 2 documents these comparisons. While we find our common uncertainty factor (positively) correlates with all the above-mentioned measures, correlation is stronger with the JLN Macro and LMN Real uncertainty indices. This is perhaps not too surprising, given that we extract uncertainty from real activity data, which have different characteristics from financial and news data. In this sense, taking our common uncertainty measure as an indicator of uncertainty in the goods sector as a whole, Figure 2 then suggests that broader uncertainty in such a sector has a component that moves in line with macroeconomic uncertainty.

Figure 2: Common and Other Measures of Uncertainty
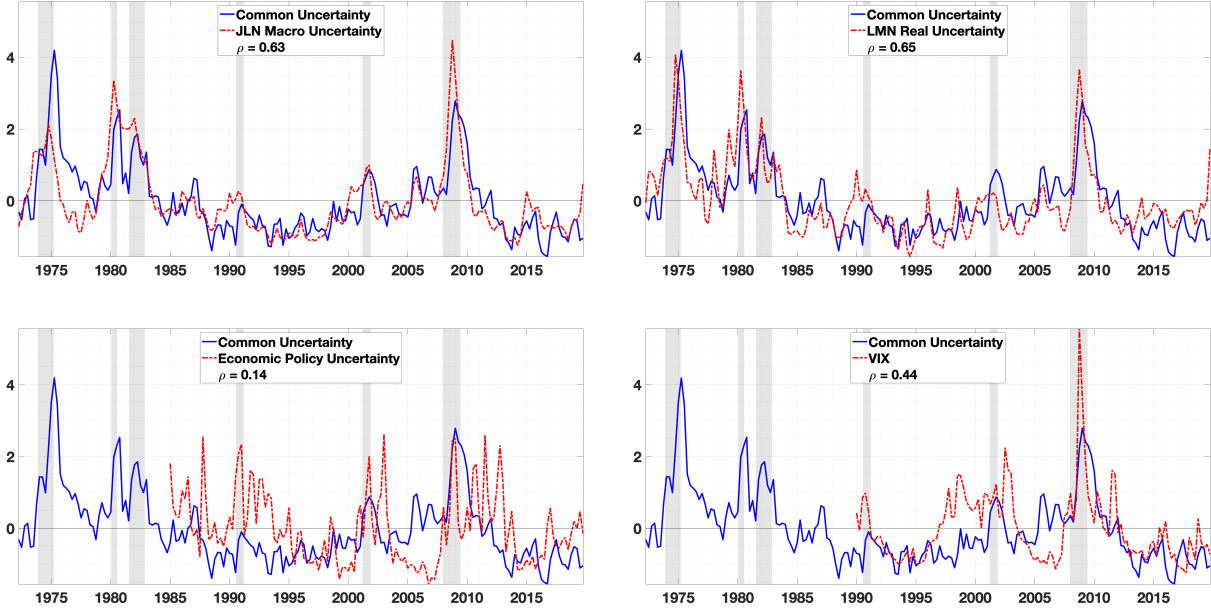
*Notes*: JLN Macro denotes uncertainty as estimated by Jurado et al. (2015). LMN Real denotes uncertainty as in Ludvigson et al. (2021). Economic Policy denotes uncertainty as as in Baker et al. (2016). VIX is the Financial Volatility Index produced by the Chicago Board Options Exchange. Measures are normalized for ease of comparison. ρ stands for the unconditional correlation coefficient between two measures of uncertainty. The vertical shaded bars correspond to NBER recession dates.

4.2 Sectoral Uncertainty

We now turn to our results for sectoral uncertainty. Figure 3 shows our measures of uncertainty that are specific to the durable and nondurable goods sectors. The two series exhibit different dynamics, which is manifested in the weak correlation (0.20) between them. Like common uncertainty, nondurable uncertainty displays its highest peak during the mid-1970s recession, suggesting that the first oil crisis of the 1970s also had repercussions at the sector-specific level in addition to its economy-wide effects. Interestingly, nondurable uncertainty is relatively stable without any discernible peaks over the remainder of our sample. This is consistent with nondurable consumption often being characterized by its excess smoothness (see, e.g., Luengo-Prado (2006)). Durable uncertainty, on the other hand, peaks during most recessions, the exception being the early-1990s recession.

Figure 3: Sectoral Uncertainty
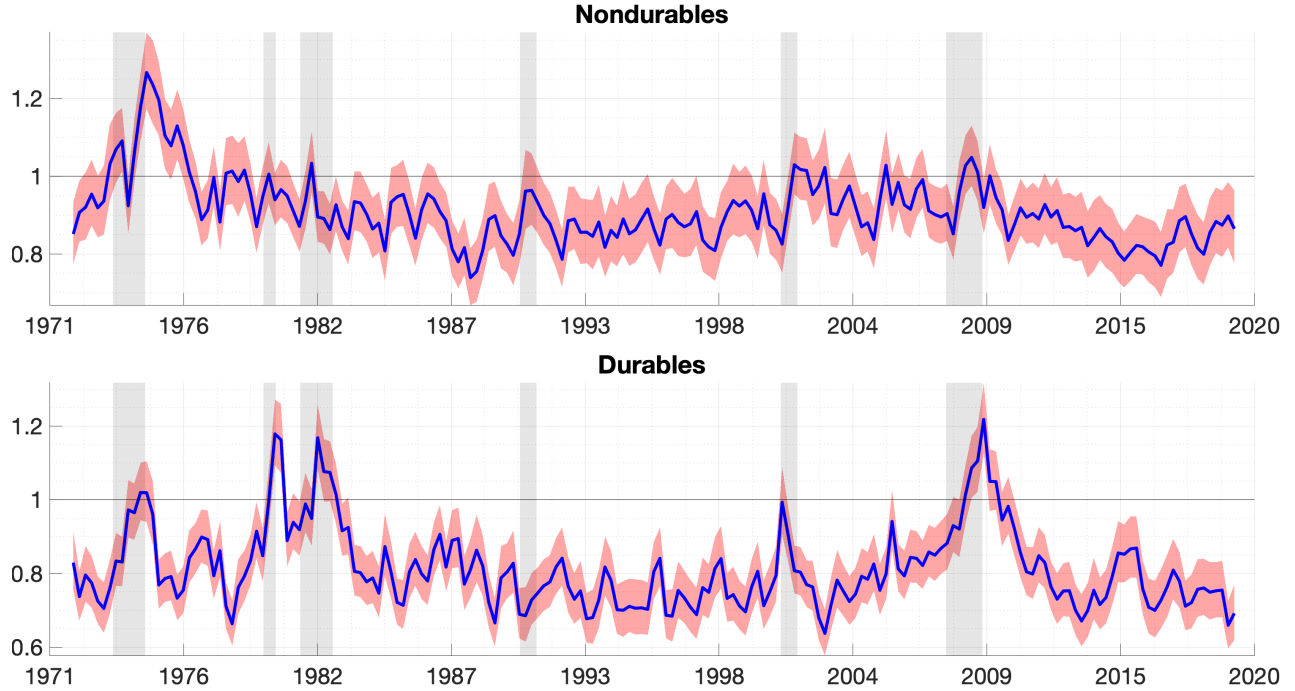
Notes: Nondurable and durable uncertainty are obtained from two subsets of disaggregated IP data consisting of 80 and 105 industries in the nondurable and durable goods sectors, respectively. The series are estimated using the methodology discussed in Sections 2 and 3. Solid lines denote the posterior median for $\exp(v_{nd,t}/2)$ (nondurables) and $\exp(v_{d,t}/2)$ (durables). Shaded regions around solid lines denote the 67% equal-tailed posterior credible interval. Vertical shaded bars correspond to NBER recession dates.

Also, unlike nondurable and common uncertainty, durable uncertainty exhibits its highest peak during the Great Recession of 2008–09, reflecting the disproportionate impact this recession had on durable-spending decisions. Such a result also echoes panel-based evidence, as documented by Berger and Vavra (2015), on the sluggish readjustment of durable expenditure to economic stimulus during the Great Recession, hence potentially exacerbating nondurable uncertainty.

Table 1 reports the correlation between our measures of uncertainty, both common and sectoral, and other macroeconomic indicators of real activity. A few results stand out. First, our common uncertainty measure is clearly countercyclical, as indicated by the negative correlation with the growth rate of variables such as real GDP, IP, and employment and the positive correlation with the NBER recession indicator. Furthermore, as pointed

out above, common uncertainty has a high positive correlation with the JLN Macro and LMN Real uncertainty measures, while somewhat less (positively) correlated with financial uncertainty measures such as the financial uncertainty index by Ludvigson et al. (2021) and the VIX.[18]

Table 1: Correlation between Our Proposed Measures of Uncertainty and Selected Economic Indicators.

Variable	Common	Nondurables	Durables
Real GDP	-0.23	-0.12	-0.19
Industrial Production	-0.30	-0.14	-0.26
Investment	-0.24	-0.12	-0.19
Employment	-0.37	-0.15	-0.38
Real PCE	0.33	0.29	0.20
CPI-Inflation	0.23	0.23	0.12
NBER Recession Indicator	0.55	0.28	0.51
JLN Macroeconomic Uncertainty	0.63	0.32	0.60
LMN Real Uncertainty	0.65	0.39	0.53
LMN Financial Uncertainty	0.36	0.24	0.29
Economic Policy Uncertainty	0.14	0.09	0.11
Monetary Policy Uncertainty	0.07	0.09	0.02
Fiscal Policy Uncertainty	0.13	0.08	0.10
VIX	0.44	0.28	0.35

Notes: The first five series above are measured as annualized growth rates.

Among the sectoral uncertainty measures, the one associated with durables is more tightly correlated with real activity indicators than nondurable uncertainty. This evidence is in line with the micro-data analysis by Kehrig (2015), who finds a more pronounced countercyclical pattern of productivity dispersion in durable goods industries than in nondurable goods industries. Also, uncertainty (common and sectoral) is positively correlated with consumer price index (CPI) inflation and real personal consumption expenditure (PCE) growth. The former correlation is consistent with firms changing their prices upward in presence of uncertainty, a mechanism known as "upward pricing bias" (Fernández-Villaverde et al., 2015; Born and Pfeifer, 2021). The positive correlation with personal consumption is consistent with closed economy models of the business cycle in which the "wait-and-see" channel—combined with the time-to-build assumption that implies a lagged impact

---

[18]Our framework also allows us to construct a measure of uncertainty by taking the average of volatilities of all industries, which would be more akin to the JLN uncertainty measure. As a matter of fact, this average measure is slightly more countercyclical and more correlated with the JLN measure.

of investment on productive capital—implies an increase in households' spending (see, e.g., Bloom et al. (2018)).

4.3 Sectoral Uncertainty and Macroeconomic Dynamics

The empirical literature has predominantly found contractionary effects after surprise increases in various (economy-wide) uncertainty measures (see, e.g., Bloom (2009), Bachmann et al. (2013), Jurado et al. (2015), and Caldara et al. (2016)). But there is no evidence if these results hold when the separation between common and sectoral uncertainty is considered. To address this, we revisit the VAR model in Jurado et al. (2015) to measure the real macroeconomic effects of our sectoral uncertainty measures. Like the authors, our vector of macroeconomic indicators is given by $\widetilde{Y}_M$=[IP, EMP, CON, PCE, NOR, WAGE, HOURS, FFR, SP500, M2]′, where we use IP as short notation for real (aggregate) industrial production, EMP for employment, CON for real consumption, PCE for PCE deflator, NOR for real new orders, WAGE for real wage, HOURS for hours, FFR for the federal funds rate, SP500 for the Standard & Poor's stock market 500 index, and M2 for money supply. The variables IP, EMP, CON, PCE, NOR, WAGE, and SP500 enter the model in log-levels, while M2 is in growth rates.

Our uncertainty measures are appended to $\widetilde{Y}_M$ and we then run three different VARs with the following vectors of endogenous variables: $\widetilde{Y}_C = [\widetilde{Y}_M', \ \exp(v_{c,t}/2)]'$, $\widetilde{Y}_{ND} = [\widetilde{Y}_M', \ \exp(v_{c,t}/2), \ \exp(v_{nd,t}/2)]'$, and $\widetilde{Y}_D = [\widetilde{Y}_M', \ \exp(v_{c,t}/2), \ \exp(v_{d,t}/2)]'$. In the first VAR, we place our proxy for common uncertainty $\exp(v_{c,t}/2)$ last, whereas for the other two VARs sectoral uncertainty measures $\exp(v_{nd,t}/2)$ and $\exp(v_{d,t}/2)$ are positioned last in the vector, right after the common uncertainty measure. Similar to Jurado et al. (2015), we orthogonalize the VAR residuals via a Cholesky decomposition of their covariance matrix. Hence, we focus on impulse responses to unexpected changes in our uncertainty measures— for brevity, we label such changes as "shocks." For future reference, the results associated with common uncertainty come from the VAR model with $\widetilde{Y}_C$, while those associated with nondurables and durables uncertainty are based on the VAR models with $\widetilde{Y}_{ND}$ and $\widetilde{Y}_D$, respectively. All VARs are estimated using Bayesian methods with the Minnesota prior of Doan et al. (1984).

Figure 4: Responses of Real Activity to Uncertainty Shocks. Full Sample: 1972Q1–2019Q4.
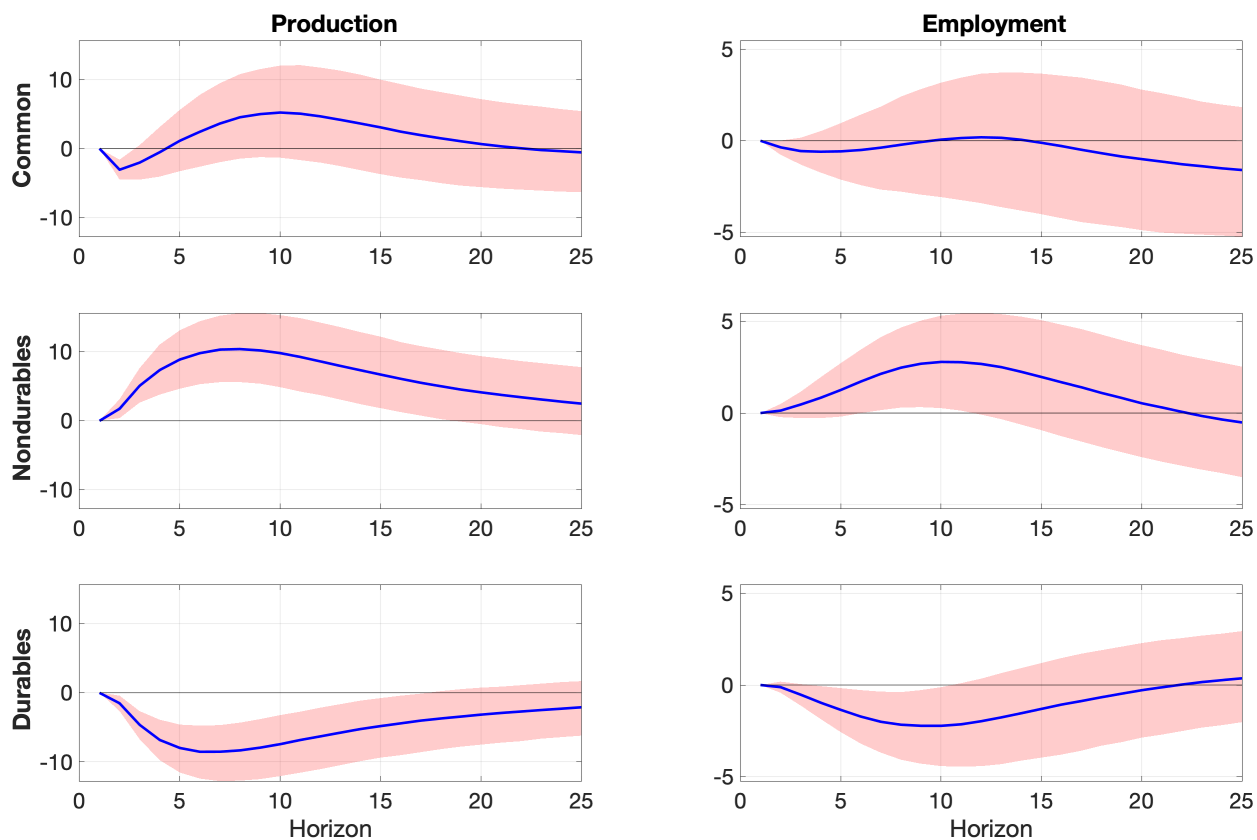
Notes: Impulse responses denote a one standard deviation shock to the common, nondurables, and durables uncertainty measures. Solid lines denote posterior medians, and the shaded areas represent the 67% equal-tailed posterior credible interval.

Figure 4 shows the responses of production and employment to a one standard deviation surprise movement in the common and sectoral uncertainty measures. Evidently, the definition of uncertainty matters. Shocks to common uncertainty generate the well-known "drop-rebound-overshoot" dynamic response of real activity after an uncertainty shock (Bloom, 2009). A different reaction is documented after an unexpected hike in durable goods uncertainty. In this case, the response of real activity is much more gradual, reaches a trough after one year, and follows a smoother (inverse) hump-shaped path. This negative response is interpretable in terms of the "wait-and-see" behavior by firms after an uncertainty shock. Such behavior is justified by non-convex adjustment costs that make it optimal to postpone investment until the "smoke clears" (Blanchard, 2009). In sharp contrast, the response of production and employment to a nondurable uncertainty shock

is positive. One plausible explanation for this result is that industries in the nondurable goods sector are typically not characterized by non-convex adjustment costs. As discussed by Bloom (2009) and Ludvigson et al. (2021), "growth options" theories of uncertainty predict that an increase in uncertainty might lead firms to invest and hire, given that such an increase in risk—coupled with the possibility of revert back investment decisions at low costs—increases expected profits due to the shape of the profit function. Another relevant difference in the transmission of uncertainty shocks in these two sectors may be related to price rigidity. In presence of higher price rigidity in the durables good sector, the real effects of uncertainty shocks might be more recessionary. This is admittedly a conjecture because, to our knowledge, there is not yet solid evidence on the relative importance of price stickiness in the durable vs. nondurable goods sector.

4.4   Sectoral Uncertainty During the Great Moderation

Recent research has documented that the onset of the Great Moderation was accompanied by an increasing role of first-moment sectoral shocks as drivers of the business cycle (Foerster et al., 2011; Atalay, 2017; Garin et al., 2018). It is thus tempting to complete the picture and verify if second-moment sectoral shocks have also become more relevant since the mid-1980s. To this end, Figure 5 documents the impulse responses of production and employment to common, durable, and nondurable uncertainty shocks for a sample running from 1984Q1 to 2019Q4. The responses to exogenous changes in common uncertainty are broadly similar to those documented for the full sample in Figure 4. A quick visual inspection, however, shows that the peak and trough responses for the nondurables and durables cases, respectively, are slightly more pronounced when fitting the VAR to the Great Moderation sample. Table 2 confirms such results by reporting the forecast error variance decomposition results based on a 24-quarter horizon. Our estimates indicate a considerably larger contribution of both sectoral uncertainty shocks to IP and employment when the sample is truncated to the Great Moderation period.

Figure 5: Responses of Real Activity to Uncertainty Shocks. Sample: 1984Q1–2019Q4.

Notes: Impulse responses denote a one standard deviation shock to the common, nondurables, and durables uncertainty measures. Solid lines denote posterior medians, and the shaded areas represent the 67% equal-tailed posterior credible interval.
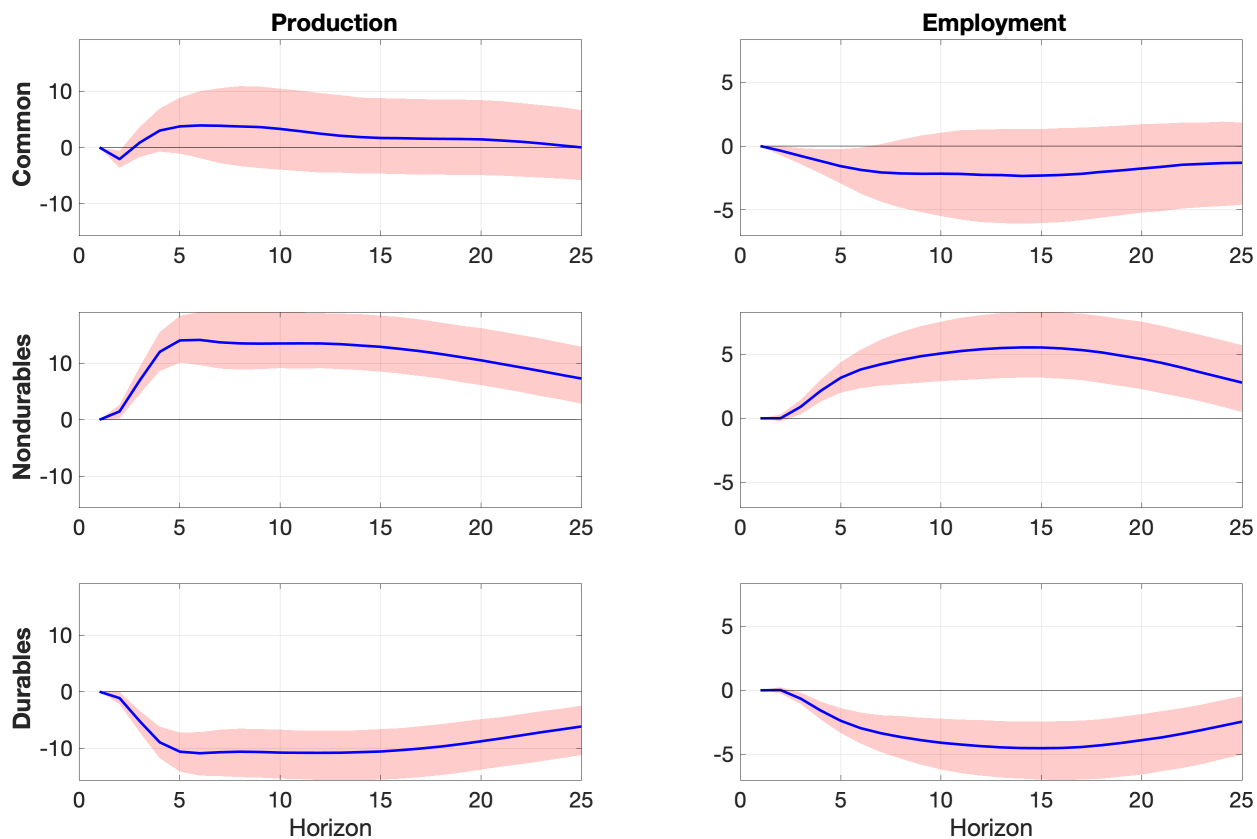
Table 2: Forecast Error Variance Decomposition (FEVD) for Uncertainty Shocks to Industrial Production and Employment.

	72Q2–19Q4	84Q1–19Q4
Ind. Production: % explained by		
Common	1.4%	1.8%
Nondurables	4.0%	11.5%
Durables	4.1%	11.9%
Employment: % explained by		
Common	1.1%	2.3%
Nondurables	1.4%	6.8%
Durables	1.5%	7.4%

Notes: FEVD results are constructed over a 24-quarter horizon.

4.5 Robustness Checks

We assess the robustness of our proposed framework along several dimensions. In particular, we generate measures of common and sectoral uncertainty under various alternative specifications for the measurement equation in (1). These include (i) four different structures for X_t; and (ii) allowing for normally (in addition to t-) distributed residuals (u_t). Regarding (i), amongst other structures, we entertain the possibility that the latent factors (i.e., f_t in (2)) exhibit conditional stochastic volatility as in, e.g., Chib et al. (2006) and Mumtaz and Musso (2019).[19]

We also examine whether our impulse-response results would hold under different VAR specifications. To this end, we recompute impulse responses from VAR models of seven macroeconomic variables (similar to Bloom (2009)) and a smaller scale VAR with five macroeconomic variables (similar to Leduc and Liu (2016) and Alessandri and Mumtaz (2019)). In the interest of space, all robustness-related results are reported in Section A2 of the Online Appendix. We do stress, however, that all our main findings carry over to the above-mentioned checks.

5 Conclusion

This paper investigates sectoral uncertainty. It does so by proposing a novel empirical framework designed to conduct the joint estimation of common uncertainty (across different sectors) and sectoral uncertainty (which is specific to selected series belonging to sectors we focus on) in a data-rich environment. We apply such a framework to 185 industrial production series for the U.S. economy. We find that durable goods uncertainty displays a large peak in correspondence with the great recession, while nondurable uncertainty was more prominent during the 1973–75 recession. Durables uncertainty is also documented to be more tightly correlated with proxies for real activity than nondurables uncertainty. Working with vector autoregressions that account for common and sectoral uncertainty, we find shocks to the former to generate a quick drop-rebound-overshoot response of real

---

[19]A model comparison exercise based on the deviance information criteria further supported the baseline specification adopted in this study to be the one with the best fit amongst all competing variants of X_t. The results for this exercise are presented in Section A2 of the Online Appendix.

activity. In contrast, shocks to durable goods uncertainty are found to generate a persistent downturn, while shocks to nondurables are expansionary. These suggest that findings in the literature that point to aggregate uncertainty as a (recessionary) driver of the business cycle might actually conflate the heterogeneous effects of common, durable, and nondurable uncertainty.

Overall, our results point to the need of investigating uncertainty at a sectoral level, both from an empirical and a theoretical standpoint. From an empirical standpoint, our contribution offers an empirical framework that encompasses frameworks successfully applied to the investigation of the role of uncertainty shocks (Carriero et al., 2016, 2018)). From a theoretical standpoint, our findings call for theoretical models featuring durable and nondurable goods and characterized by different second-moment shocks with a heterogeneous impact on the business cycle.

References

Acemoglu, Daron, Asuman Ozdaglar, and Alireza Tahbaz-Salehi, "Microeconomic origins of macroeconomic tail risks," *American Economic Review*, 2017, *107* (1), 54–108.

_ , **Vasco M Carvalho, Asuman Ozdaglar, and Alireza Tahbaz-Salehi**, "The network origins of aggregate fluctuations," *Econometrica*, 2012, *80* (5), 1977–2016.

Alessandri, Piergiorgio and Haroon Mumtaz, "Financial regimes and uncertainty shocks," *Journal of Monetary Economics*, 2019, *101*, 31–46.

Alessi, Lucia, Matteo Barigozzi, and Marco Capasso, "Improved penalization for determining the number of factors in approximate factor models," *Statistics & Probability Letters*, 2010, *80* (23-24), 1806–1813.

Angelini, Giovanni, Emanuele Bacchiocchi, Giovanni Caggiano, and Luca Fanelli, "Uncertainty across volatility regimes," *Journal of Applied Econometrics*, 2019, *34(3)*, 437–455.

Antolín-Díaz, Juan, Thomas Drechsel, and Ivan Petrella, "Advances in nowcasting economic activity: Secular trends, large shocks and new data," Technical Report, Working Paper 2020.

Atalay, Enghin, "How important are sectoral shocks?," *American Economic Journal: Macroeconomics*, 2017, *9* (4), 254–80.

Bachmann, Rüdiger, Steffen Elstner, and Eric R Sims, "Uncertainty and economic activity: Evidence from business survey data," *American Economic Journal: Macroeconomics*, 2013, *5* (2), 217–49.

Bai, Jushan and Serena Ng, "Determining the number of factors in approximate factor models," *Econometrica*, 2002, *70* (1), 191–221.

__ **and** __ , "Extremum estimation when the predictors are estimated from large panels," *Annals of Economics and Finance*, 2008, *9* (2), 201–222.

Baker, Scott R, Nicholas Bloom, and Steven J Davis, "Measuring economic policy uncertainty," *The Quarterly Journal of Economics*, 2016, *131* (4), 1593–1636.

Baqaee, David Rezza and Emmanuel Farhi, "The macroeconomic impact of microeconomic shocks: Beyond Hulten's Theorem," *Econometrica*, 2019, *87* (4), 1155–1203.

Basu, Susanto and Brent Bundick, "Uncertainty shocks in a model of effective demand," *Econometrica*, 2017, *85* (3), 937–958.

Berger, David and Joseph Vavra, "Consumption dynamics during recessions," *Econometrica*, 2015, *83* (1), 101–154.

Bianchi, Francesco, Howard Kung, and Mikhail Tirskikh, "The origins and effects of macroeconomic uncertainty," 2021, *available at https://sites.google.com/view/francescobianchi/home.*

Blanchard, O., "(Nearly) nothing to fear but fear itself," 2009, *The Economist, January 29.*

Bloom, Nicholas, "The impact of uncertainty shocks," *Econometrica*, 2009, *77* (3), 623–685.

__ , "Fluctuations in uncertainty," *Journal of Economic Perspectives*, 2014, *28* (2), 153–76.

__ , **Max Floetotto, Nir Jaimovich, Itay Saporta-Eksten, and Stephen J Terry**, "Really uncertain business cycles," *Econometrica*, 2018, *86* (3), 1031–1065.

Born, Benjamin and Johannes Pfeifer, "Uncertainty-driven business cycles: Assessing the markup channel," *Quantitative Economics*, 2021, *12(2)*, 587–623.

Caggiano, G., E. Castelnuovo, and G. Nodari, "Uncertainty and monetary policy in good and bad times: A replication of the VAR investigation by Bloom (2009)," *Journal of Applied Econometrics*, 2022, *37*, 210–217.

Caggiano, Giovanni, Efrem Castelnuovo, and Nicolas Groshenny, "Uncertainty shocks and unemployment dynamics in US recessions," *Journal of Monetary Economics*, 2014, *67*, 78–92.

Caldara, Dario, Cristina Fuentes-Albero, Simon Gilchrist, and Egon Zakrajšek, "The macroeconomic impact of financial and uncertainty shocks," *European Economic Review*, 2016, *88*, 185–207.

Carriero, Andrea, Todd E Clark, and Massimiliano Marcellino, "Common drifting volatility in large Bayesian VARs," *Journal of Business & Economic Statistics*, 2016, *34* (3), 375–390.

__ , __ , **and** __ , "Measuring uncertainty and its impact on the economy," *Review of Economics and Statistics*, 2017, (0).

__ , __ , **and** __ , "Measuring uncertainty and its impact on the economy," *Review of Economics and Statistics*, 2018, *100* (5), 799–815.

__ , **Todd E. Clark, Massimiliano Marcellino, and Elmar Mertens**, "Measuring uncertainty and its effects in the COVID-19 era," 2020, *Queen Mary - University of London, Federal Reserve Bank of*

Cleveland, Bocconi University, and Deutsche Bundesbank, mimeo.

Cascaldi-Garcia, Danilo, Cisil Sarisoy, Juan M. Londono, Bo Sun, Deepa Datta, Thiago Ferreira, Olesya Grishchenko, Mohammad R. Jahan-Parvar, Francesca Loria, Sai Ma, Marius Rodriguez, Ilknur Zer, and John Rogers, "What is certain about uncertainty?," *Journal of Economic Literature*, 2021.

Chan, J.C.C. and I. Jeliazkov, "Efficient simulation and integrated likelihood estimation in state space models," *International Journal of Mathematical Modelling and Numerical Optimisation*, 2009, *1(1-2)*, 101–120.

Chib, Siddhartha, Federico Nardari, and Neil Shephard, "Analysis of high dimensional multivariate stochastic volatility models," *Journal of Econometrics*, 2006, *134* (2), 341–371.

Choi, Sangyup and Prakash Loungani, "Uncertainty and unemployment: The effects of aggregate and sectoral channels," *Journal of Macroeconomics*, 2015, *46*, 344–358.

Clark, Todd E., Michael W. McCracken, and Elmar Mertens, "Modeling time-varying uncertainty of multiple-horizon forecast errors," *Review of Economics and Statistics*, 2020, *102* (1), 17–33.

Coibion, Olivier, Dimitris Georgarakos, Yuriy Gorodnichenko, Geoff Kenny, and Michael Weber, "The effect of macroeconomic uncertainty on household spending," 2021, *National Bureau of Economic Research Working Paper No. 28625.*

Conley, Timothy G and Bill Dupor, "A spatial analysis of sectoral complementarity," *Journal of Political Economy*, 2003, *111* (2), 311–352.

Doan, Thomas, Robert Litterman, and Christopher Sims, "Forecasting and conditional projection using realistic prior distributions," *Econometric Reviews*, 1984, *3* (1), 1–100.

Fernández-Villaverde, Jesus and Pablo Guerron-Quintana, "Uncertainty shocks in real business cycle models," *Review of Economic Dynamics*, 2020, *37*, 118–166.

_ , _ , Juan F. Rubio-Ramírez, and M. Uribe, "Risk matters: The real effects of volatility shocks," *American Economic Review*, 2011, *101(6)*, 2530–2561.

_ , _ , Keith Kuester, and Juan F. Rubio-Ramírez, "Fiscal volatility shocks and economic activity," *American Economic Review*, 2015, *105(11)*, 3352–3384.

Foerster, Andrew T, Pierre-Daniel G Sarte, and Mark W Watson, "Sectoral versus aggregate shocks: A structural factor analysis of industrial production," *Journal of Political Economy*, 2011, *119* (1), 1–38.

Galí, Jordi and Luca Gambetti, "On the sources of the great moderation," *American Economic Journal: Macroeconomics*, 2009, *1* (1), 26–57.

Garin, Julio, Michael J Pries, and Eric R Sims, "The relative importance of aggregate and sectoral shocks and the changing nature of economic fluctuations," *American Economic Journal: Macroeconomics*, 2018, *10* (1), 119–48.

Gorodnichenko, Yuriy and Serena Ng, "Level and volatility factors in macroeconomic data," *Journal*

of Monetary Economics, 2017, *91*, 52–68.

Hoke, Sinem Hacioglu and Kerem Tuzcuoglu, "Interpreting the latent dynamic factors by threshold FAVAR model," *Staff Working Paper Series 622, Bank of England*, 2016.

Horvath, Michael, "Cyclicality and sectoral linkages: Aggregate fluctuations from independent sectoral shocks," *Review of Economic Dynamics*, 1998, *1* (4), 781–808.

_ , "Sectoral shocks and aggregate fluctuations," *Journal of Monetary Economics*, 2000, *45* (1), 69–106.

Jacquier, Eric, Nicholas G Polson, and Peter E Rossi, "Bayesian analysis of stochastic volatility models with fat-tails and correlated errors," *Journal of Econometrics*, 2004, *122* (1), 185–212.

Jo, Soojin and Rodrigo Sekkel, "Macroeconomic uncertainty through the lens of professional forecasters," *Journal of Business & Economic Statistics*, 2019, *37* (3), 436–446.

Jurado, Kyle, Sydney C Ludvigson, and Serena Ng, "Measuring uncertainty," *American Economic Review*, 2015, *105* (3), 1177–1216.

Kehoe, Patrick J, Virgiliu Midrigan, and Elena Pastorino, "Evolution of modern business cycle models: Accounting for the great recession," *Journal of Economic Perspectives*, 2018, *32* (3), 141–66.

Kehrig, Matthias, "The cyclical nature of the productivity distribution," *Earlier version: US Census Bureau Center for Economic Studies Paper No. CES-WP-11-15*, 2015.

Kim, Sangjoon, Neil Shephard, and Siddhartha Chib, "Stochastic volatility: Likelihood inference and comparison with ARCH models," *Review of Economic Studies*, 1998, *65(3)*, 361–393.

Kim, Yunmi and Chang-Jin Kim, "Dealing with endogeneity in a time-varying parameter model: Joint estimation and two-step estimation procedures," *The Econometrics Journal*, 2011, *14* (3), 487–497.

Koop, Gary, Dale J. Poirier, and Justin L. Tobias, "Bayesian econometric methods," 2007, *Cambridge University Press*.

Kose, M Ayhan, Christopher Otrok, and Charles H Whiteman, "International business cycles: World, region, and country-specific factors," *American Economic Review*, 2003, *93* (4), 1216–1239.

Kroese, Dirk P. and Joshua C.C. Chan, "Statistical modeling and computation," 2014, *Springer, New York, NY.*

Leduc, Sylvain and Zheng Liu, "Uncertainty shocks are aggregate demand shocks," *Journal of Monetary Economics*, 2016, *82(C)*, 20–35.

Lenza, Michele and Giorgio Primiceri, "How to estimate a VAR after March 2020," *Journal of Applied Econometrics*, 2021, *forthcoming.*

Ludvigson, Sydney C and Serena Ng, "Macro factors in bond risk premia," *The Review of Financial Studies*, 2009, *22* (12), 5027–5067.

Ludvigson, Sydney C., Sai Ma, and Serena Ng, "Uncertainty and business cycles: Exogenous impulse or endogenous response?," *American Economic Journal: Macroeconomics*, 2021, *13(4)*, 369–410.

Luengo-Prado, María José, "Durables, nondurables, down payments and consumption excesses," *Journal of Monetary Economics*, 2006, *53* (7), 1509–1539.

Ma, Xiaohan and Roberto Samaniego, "Deconstructing uncertainty," *European Economic Review*, 2019, *119*, 22–41.

Marcellino, Massimiliano, Todd Clark, and Andrea Carriero, "Nowcasting tail risk to economic activity at a weekly frequency," 2021, *CEPR Discussion Paper No. 16496.*

McCausland, William J., Shirley Millera, and Denis Pelletierc, "Simulation smoothing for state-space models: A computational efficiency analysis," *Computational Statistics and Data Analysis*, 2011, *55*, 199–212.

McCracken, Michael W. and Serena Ng, "FRED-MD: A monthly database for macroeconomic research," *Journal of Business and Economic Statistics*, 2016, *34(4)*, 574–589.

Miron, Jeffrey A and Stephen P Zeldes, "Production, sales, and the change in inventories: An identity that doesn't add up," *Journal of Monetary Economics*, 1989, *24* (1), 31–51.

Moench, Emanuel, Serena Ng, and Simon Potter, "Dynamic hierarchical factor models," *Review of Economics and Statistics*, 2013, *95* (5), 1811–1817.

Mumtaz, Haroon and Alberto Musso, "The evolving impact of global, region-specific, and country-specific uncertainty," *Journal of Business & Economic Statistics*, 2019, pp. 1–16.

Negro, Marco Del and Christopher Otrok, "99 Luftballons: Monetary policy and the house price boom across US states," *Journal of Monetary Economics*, 2007, *54* (7), 1962–1985.

_ and Giorgio E Primiceri, "Time varying structural vector autoregressions and monetary policy: A corrigendum," *The Review of Economic Studies*, 2015, *82* (4), 1342–1345.

Omori, Yasuhiro, Siddhartha Chib, Neil Shephard, and Jouchi Nakajima, "Stochastic volatility with leverage: Fast and efficient likelihood inference," *Journal of Econometrics*, 2007, *140(2)*, 425–449.

Pagan, Adrian, "Econometric issues in the analysis of regressions with generated regressors," *International Economic Review*, 1984, pp. 221–247.

Segal, Gill, "A tale of two volatilities: Sectoral uncertainty, growth, and asset prices," *Journal of Financial Economics*, 2019.

Sims, Christopher A. and Tao Zha, "Were there regime switches in U.S. monetary policy?," *American Economic Review*, 2006.

Stock, James H and Mark W Watson, "Has the business cycle changed and why?," *NBER Macroeconomics Annual*, 2002, *17*, 159–218.

Stock, James H. and Mark W. Watson, "Dynamic factor models, factor-augmented vector autoregressions, and structural vector autoregressions in macroeconomics," 2016, *in: J. B. Taylor and H. Uhlig (Eds.): Handbook of Macroeconomics, Vol. 2, North Holland*, 415–525.

Wynne, Mark A and Nathan S Balke, "Recessions and recoveries," *Federal Reserve Bank of Dallas, Economic Review, first quarter*, 1993, pp. 1–18.

Online Appendix to
Sectoral Uncertainty [*]

Efrem Castelnuovo[†]   Kerem Tuzcuoglu[‡]   Luis Uzeda[§]

Contents

A1   Estimation Details

For convenience, below we reproduce the stacked representation of our model as presented in Section 3.2 of the main text:

$$\mathbf{y} = \mathbf{X}\boldsymbol{\beta} + \mathbf{L}_\Psi \mathbf{L}_h \mathbf{e} \quad \mathbf{e} \sim \mathcal{N}\left(\mathbf{0},\ I_{NT}\right) \tag{A1}$$

$$\mathbf{h} = \boldsymbol{\Lambda}\mathbf{v}, \tag{A2}$$

$$\mathbf{L}_{\Phi_v}\mathbf{v} = \widetilde{\mathbf{v}}_0 + \boldsymbol{\eta_v} \quad \mathbf{v} \sim \mathcal{N}\left(\mathbf{0},\ \boldsymbol{\Sigma_v}\right), \tag{A3}$$

where:

$$\mathbf{X} = \begin{bmatrix} I_N \otimes z_1' & I_N \otimes f_1' \\ \vdots & \vdots \\ I_N \otimes z_T' & I_N \otimes f_T' \end{bmatrix}, \quad \boldsymbol{\beta} = \begin{bmatrix} \boldsymbol{\beta}_z \\ \boldsymbol{\beta}_f \end{bmatrix}, \quad \boldsymbol{\Lambda} = I_T \otimes \begin{bmatrix} \Lambda^c & \Lambda^s \end{bmatrix},$$

$$\mathbf{L}_h = \mathtt{diag}\left(\Sigma_1^{\frac{1}{2}}, \cdots, \Sigma_T^{\frac{1}{2}}\right), \quad \mathbf{L}_\Psi = \mathtt{diag}\left(\Psi_1^{\frac{1}{2}}, \cdots, \Psi_T^{\frac{1}{2}}\right), \quad \mathbf{L}_{\Phi_v} = \begin{bmatrix} I_3 & \mathbf{0} & \cdots & & \mathbf{0} \\ -\Phi_v & I_3 & & & \\ \mathbf{0} & -\Phi_v & \ddots & & \vdots \\ \vdots & & \ddots & & \\ \mathbf{0} & & \cdots & -\Phi_v & I_3 \end{bmatrix},$$

$\boldsymbol{\Sigma_v} = I_T \otimes \mathtt{diag}(\sigma_{v_c}^2,\ \sigma_{v_d}^2,\ \sigma_{v_{nd}}^2)$, and the vector $\widetilde{\mathbf{v}}_0 = \iota_0 \otimes (\Phi_v v_0)$ collects the initial conditions for the common and sectoral uncertainty measures. ι_0 denotes a $T \times 1$ vector given by $\iota_0 = (1,\ 0, \cdots, 0)'$.

Next, recall from our discussion in Section 2 that z_t denotes a vector collecting the principal components (seven in total) extracted from a large set of macroeconomic indicators (i.e., the FRED-MD database). These are obtained following the same approach as in McCracken and Ng (2016). The other set of controls, f_t, denote a vector collecting latent dynamic factors (four in total) extracted from the 185 industries in our IP dataset. We define f_t as the vector collecting IP-specific factors. These are jointly modeled as a VAR(1)

process, i.e.:

$$f_t = \Phi_f f_{t-1} + \eta_{f,t}, \quad \eta_{f,t} \sim \mathcal{N}\left(0, \ \mathtt{diag}\left(\sigma_{f_1}^2, \cdots, \sigma_{f_4}^2\right)\right). \tag{A4}$$

A1.1   Posterior Sampler

Let the parameters and states in our model be, respectively, organized into the following sets: $\boldsymbol{\theta} = \{\tilde{\boldsymbol{\beta}}_z, \ \tilde{\boldsymbol{\beta}}_f, \ \tilde{\boldsymbol{\lambda}}_c, \ \tilde{\boldsymbol{\lambda}}_d, \ \tilde{\boldsymbol{\lambda}}_{nd}, \ \boldsymbol{\phi}_{\mathbf{f}}, \ \boldsymbol{\phi}_{\mathbf{v}}, \ \boldsymbol{\sigma}_{\mathbf{f}}^2, \ \boldsymbol{\sigma}_{\mathbf{v}}^2\}$ and $\mathcal{Z} = \{\boldsymbol{\psi}, \ \mathbf{f}, \ \mathbf{v}\}$.[1] Posterior draws are generated by sampling sequentially from:

$$\mathtt{MCMC\ Steps:} \begin{cases} p\left(\mathbf{f}|\mathbf{y}, \mathcal{Z}_{-\mathbf{f}}, \boldsymbol{\theta}\right), \\[4pt] p\left(\boldsymbol{\psi}|\mathbf{y}, \mathcal{Z}_{-\boldsymbol{\psi}}, \boldsymbol{\theta}\right), \\[4pt] p\left(\mathbf{v}|\mathbf{y}, \mathcal{Z}_{-\mathbf{v}}, \boldsymbol{\theta}\right), \\[4pt] p\left(\tilde{\boldsymbol{\beta}}_x|\mathbf{y}, \mathcal{Z}, \boldsymbol{\theta}_{-\tilde{\beta}_x}\right) \quad \text{for } x = z, \ f, \\[4pt] p\left(\tilde{\boldsymbol{\lambda}}_j|\mathbf{y}, \mathcal{Z}, \boldsymbol{\theta}_{-\tilde{\lambda}_j}\right) \quad \text{for } j = c, \ d, \ nd, \\[4pt] p\left(\boldsymbol{\phi}_{\boldsymbol{\ell}}|\mathbf{y}, \mathcal{Z}, \boldsymbol{\theta}_{-\phi_{\boldsymbol{\ell}}}\right), \\[4pt] p\left(\boldsymbol{\sigma}_{\boldsymbol{\ell}}^2|\mathbf{y}, \mathcal{Z}, \boldsymbol{\theta}_{-\sigma_{\boldsymbol{\ell}}^2}\right) \quad \text{for } \boldsymbol{\ell} = \mathbf{v}, \ \mathbf{f}. \end{cases} \tag{A5}$$

In what follows we provide a detailed discussion on each of the steps above. For ease of exposition, we separate the discussion below into two parts, namely state simulation (i.e., the first three conditional posterior densities) and parameter sampling (i.e., the last four densities).

A1.1.1   State Simulation

(i) Drawing the IP-specific factors

Let $\mathbf{f} = (f_1, \cdots, f_T)'$ and $\mathbf{z} = (z_1, \cdots, z_T)'$ denote the stacked representation for the IP-specific and McCracken and Ng (2016) factors, respectively. By a simple change of variable,

---

[1]A detailed description of each element in these sets is provided in Sections 3.1 and 3.2 of the main text.

we can recast the controls in (A1) as $\mathbf{X}\boldsymbol{\beta} = \mathbf{X}_{\beta_f}\mathbf{f} + \mathbf{X}_{\beta_z}\mathbf{z}$. This yields:

$$\mathbf{y_f} = \mathbf{X}_{\beta_f}\mathbf{f} + \mathbf{u} \qquad \mathbf{u} \sim \mathcal{N}\left(\mathbf{0},\ \boldsymbol{\Sigma}_u\right), \tag{A6}$$

where:

$$\mathbf{y_f} = \mathbf{y} - \mathbf{X}_{\beta_z}\mathbf{z}, \quad \mathbf{u} = \mathbf{L}_\Psi \mathbf{L}_h \mathbf{e}, \quad \boldsymbol{\Sigma}_u = \mathbf{L}_\Psi \mathbf{L}_h \mathbf{L}'_h \mathbf{L}'_\Psi, \quad \mathbf{X}_{\beta_j} = I_T \otimes \Lambda_{\beta_x} \quad \text{for } x = z,\ f,$$

$$\Lambda_{\beta_z} = \begin{bmatrix} \beta^z_{1,1} & \cdots & \beta^z_{7,1} \\ \vdots & \vdots & \vdots \\ \beta^z_{1,N} & \cdots & \beta^z_{7,N} \end{bmatrix}, \quad \Lambda_{\beta_f} = \begin{bmatrix} \beta^f_{1,1} & \cdots & \beta^f_{4,1} \\ \vdots & \vdots & \vdots \\ \beta^f_{1,N} & \cdots & \beta^f_{4,N} \end{bmatrix}.$$

Next, from (A4) we obtain the following stacked representation for $\mathbf{f}$:

$$\mathbf{L}_{\Phi_f}\mathbf{f} = \widetilde{\mathbf{f}}_0 + \boldsymbol{\eta_f} \qquad \boldsymbol{\eta_f} \sim \mathcal{N}\left(\mathbf{0},\ \boldsymbol{\Sigma_f}\right), \tag{A7}$$

where:

$$\mathbf{L}_{\Phi_f} = \begin{bmatrix} I_4 & \mathbf{0} & \cdots & & \mathbf{0} \\ -\Phi_f & I_4 & & & \\ \mathbf{0} & -\Phi_f & \ddots & & \vdots \\ \vdots & & \ddots & & \\ \mathbf{0} & & \cdots & -\Phi_f & I_4 \end{bmatrix}, \quad \widetilde{\mathbf{f}}_0 = \iota_0 \otimes (\Phi_f f_0), \quad \boldsymbol{\Sigma_f} = I_T \otimes \mathtt{diag}\left(\sigma^2_{f_1}, \cdots, \sigma^2_{f_4}\right),$$

such that ι_0 denotes a $T \times 1$ vector given by $\iota_0 = (1,\ 0, \cdots, 0)'$ and $\sigma^2_{f_i}$ for $i = 1, \cdots, 4$ denotes the variance of the ith innovation driving the ith IP-specific factor. Combining (A6)–(A7) and applying standard linear regression results yields:

$$\mathbf{f}|\mathbf{y}, \mathcal{Z}_{-\mathbf{f}}, \boldsymbol{\theta} \sim \mathcal{N}\left(\overline{\mathbf{d}}_\mathbf{f},\ \overline{\mathbf{D}}_\mathbf{f}\right), \quad \text{where} \quad \begin{cases} \overline{\mathbf{d}}_\mathbf{f} = \overline{\mathbf{D}}_\mathbf{f}\left(\mathbf{X}'_{\beta_f}\boldsymbol{\Sigma}_u^{-1}\mathbf{y_f} + \mathbf{L}'_{\Phi_f}\boldsymbol{\Sigma_f}^{-1}\widetilde{\mathbf{f}}_0\right), \\ \overline{\mathbf{D}}_\mathbf{f} = \left(\mathbf{X}'_{\beta_f}\boldsymbol{\Sigma}_u^{-1}\mathbf{X}_{\beta_f} + \boldsymbol{\Sigma_f}^{-1}\right)^{-1}. \end{cases} \tag{A8}$$

Note that to construct $\overline{\mathbf{D}}_\mathbf{f}$ one is required to invert an $NT \times NT$ matrix. Carrying out

such an operation via brute-force methods is computationally cumbersome. Therefore, we adopt a more efficient approach suggested by Chan and Jeliazkov (2009), often referred to as precision sampling. To illustrate how we employ their method, we first introduce the following notation: given a lower triangular $NT \times NT$ non-singular matrix $\mathbf{C}$ and a $NT \times 1$ vector $\mathbf{b}$, let $\mathbf{C} \backslash \mathbf{b}$ denote the unique solution to the triangular system $\mathbf{C}\mathbf{x} = \mathbf{b}$ obtained by forward substitution, i.e., $\mathbf{x} = \mathbf{C} \backslash \mathbf{b} = \mathbf{C}^{-1}\mathbf{b}$. Sampling $\mathbf{f}$ is then conducted by following the four operations below:

$$
\begin{aligned}
(1) \quad &Chol(\overline{\mathbf{D}}_{\mathbf{f}}^{-1}) = \mathbf{CC}', \\
(2) \quad &\mathbf{x} = \mathbf{C} \backslash \left(\mathbf{X}'_{\beta_f} \boldsymbol{\Sigma}_u^{-1} \mathbf{y}_{\mathbf{f}} + \mathbf{L}'_{\Phi_f} \boldsymbol{\Sigma}_{\mathbf{f}}^{-1} \widetilde{\mathbf{f}}_0 \right), \\
(3) \quad &\overline{\mathbf{d}}_{\mathbf{f}} = \mathbf{C}' \backslash \mathbf{x}, \\
(4) \quad &\mathbf{f} = \overline{\mathbf{d}}_{\mathbf{f}} + \mathbf{C}' \backslash \boldsymbol{\zeta} \qquad \boldsymbol{\zeta} \sim \mathcal{N}\left(\mathbf{0}, \ I_{NT}\right).
\end{aligned}
$$

The first step describes the Cholesky decomposition of the inverse covariance (or precision) matrix $\overline{\mathbf{D}}_{\mathbf{f}}^{-1}$. Step 2 requires solving a triangular system by forward substitution, given that $\mathbf{C}$ is a lower triangular matrix. Step 3 is analogous to Step 2, except that the solution of the triangular system, $\mathbf{C}' \backslash \mathbf{x}$, is now obtained by backward substitution, since $\mathbf{C}'$ is an upper triangular matrix. It is then straightforward to see that Steps 2 and 3 combined, by construction, yield:

$$
\begin{aligned}
\overline{\mathbf{d}}_{\mathbf{f}} &= \mathbf{C}'^{-1}\left(\mathbf{C}^{-1} \left(\mathbf{X}'_{\beta_f} \boldsymbol{\Sigma}_u^{-1} \mathbf{y}_{\mathbf{f}} + \mathbf{L}'_{\Phi_f} \boldsymbol{\Sigma}_{\mathbf{f}}^{-1} \widetilde{\mathbf{f}}_0 \right) \right) = (\mathbf{CC}')^{-1}\left(\mathbf{X}'_{\beta_f} \boldsymbol{\Sigma}_u^{-1} \mathbf{y}_{\mathbf{f}} + \mathbf{L}'_{\Phi_f} \boldsymbol{\Sigma}_{\mathbf{f}}^{-1} \widetilde{\mathbf{f}}_0 \right) \\
&= \overline{\mathbf{D}}_{\mathbf{f}} \left(\mathbf{X}'_{\beta_f} \boldsymbol{\Sigma}_u^{-1} \mathbf{y}_{\mathbf{f}} + \mathbf{L}'_{\Phi_f} \boldsymbol{\Sigma}_{\mathbf{f}}^{-1} \widetilde{\mathbf{f}}_0 \right).
\end{aligned}
$$

Finally, Step 4 describes an affine transformation of a standard normal random vector that ensures, by definition, that the expression in such a step returns a $NT \times 1$ random vector $\mathbf{f}|\mathbf{y}, \mathcal{Z}_{-\mathbf{f}}, \boldsymbol{\theta} \sim \mathcal{N}\left(\overline{\mathbf{d}}_{\mathbf{f}}, \ \overline{\mathbf{D}}_{\mathbf{f}}\right)$.

- *Initial Conditions*

We treat the vector containing the state initialization conditions (i.e., f_0) as an additional parameter to our model. We thus extend our MCMC algorithm to sample f_0. Accordingly,

we rewrite (A7) as:

$$\mathbf{L}_{\Phi_f}\mathbf{f} = \mathbf{L}_{0f}f_0 + \boldsymbol{\eta_f} \qquad \boldsymbol{\eta_f} \sim \mathcal{N}\left(\mathbf{0},\ \boldsymbol{\Sigma_f}\right), \tag{A9}$$

where:

$$\mathbf{L}_{0f} = \begin{bmatrix} \Phi_f \\ 0 \times I_4 \\ \vdots \\ 0 \times I_4 \end{bmatrix}.$$

Assuming a Gaussian prior $f_0 \sim \mathcal{N}\left(\hat{\boldsymbol{\mu}}_{f_0},\ \hat{\boldsymbol{\Sigma}}_{f_0}\right)$ and using standard regression results gives:

$$f_0|\mathbf{y}, \mathcal{Z}, \boldsymbol{\theta} \sim \mathcal{N}\left(\overline{\mathbf{d}}_{f_0},\ \overline{\mathbf{D}}_{f_0}\right),\ \text{ where } \begin{cases} \overline{\mathbf{d}}_{f_0} = \overline{\mathbf{D}}_{f_0}\left(\mathbf{L}'_{0f}\boldsymbol{\Sigma}_{\mathbf{f}}^{-1}\mathbf{L}_{\Phi_f}\mathbf{f} + \hat{\boldsymbol{\Sigma}}_{f_0}^{-1}\hat{\boldsymbol{\mu}}_{f_0}\right), \\ \overline{\mathbf{D}}_{f_0} = \left(\mathbf{L}'_{0f}\boldsymbol{\Sigma}_{\mathbf{v}}^{-1}\mathbf{L}_{0f} + \hat{\boldsymbol{\Sigma}}_{f_0}^{-1}\right)^{-1}. \end{cases} \tag{A10}$$

(ii) Drawing the outlier-adjustment component

Recall from Section 2.3 that we elicit an inverse-gamma prior to (the square of) each element in the scale matrix $\Psi_t^{\frac{1}{2}} = \texttt{diag}\left(\psi_{1,t}^{\frac{1}{2}}, \cdots, \psi_{N,t}^{\frac{1}{2}}\right)$ collected by $\mathbf{L}_{\Psi} = \texttt{diag}\left(\Psi_1^{\frac{1}{2}}, \cdots, \Psi_T^{\frac{1}{2}}\right)$, i.e.:

$$\psi_{i,t} \overset{i.i.d.}{\sim} \mathcal{IG}\left(\frac{\nu_\psi}{2}, \frac{\nu_\psi}{2}\right) \text{ for } i = 1, \cdots, N \text{ and } t = 1, \cdots, T. \tag{A11}$$

Since $\psi_{1,1}, \cdots, \psi_{N,T}$ are conditionally independent given the model parameters, states, and the data, we can draw each of them sequentially from the natural-conjugate inverse-gamma conditional posterior. In other words, we have:

$$\psi_{i,t}|\mathbf{y}, \mathcal{Z}, \boldsymbol{\theta}_{-\psi_{i,t}} \sim \mathcal{IG}\left(\overline{\nu}_{i,t}^\psi,\ \overline{S}_{i,t}^\psi\right),\ \text{ where } \begin{cases} \overline{\nu}_{i,t}^\psi = \frac{\nu_\psi + 1}{2}, \\ \overline{S}_{i,t}^\psi = \frac{\tilde{e}_{i,t}^2 + \nu_\psi}{2} \quad \text{for } i = 1, \cdots, 7 \text{ and } t = 1, \cdots, T, \end{cases} \tag{A12}$$

and $\tilde{e}_{i,t}$ denotes each element in the $NT \times 1$ vector of innovations given by $\tilde{\mathbf{e}} = \mathbf{L}_h\mathbf{e}$.

5

(iii) **Drawing the common and sector-specific uncertainty factors**

Recall from Section 3.2 that to sample $\mathbf{v}$ we adopt the auxiliary mixture-sampling approach by Omori et al. (2007). This entails a two-step procedure:

Step 1 $p(\mathbf{k}|\widetilde{\mathbf{y}}^*, \mathcal{Z}, \boldsymbol{\theta})$ $s.t.$ $\mathbf{k} = (k_1, \cdots, k_T)$,

Step 2 $p(\mathbf{v}|\widetilde{\mathbf{y}}^*, \mathcal{Z}_{-\mathbf{v}}, \mathbf{k}, \boldsymbol{\theta})$.

●Step 1

Each element of $\mathbf{k} = (k_1, \cdots, k_T)$ is drawn independently from a multinomial distribution parameterized by the full conditional posterior probabilities $\mathrm{Pr}\left(k_t = i|\widetilde{y}^*_{\tau,t}, z_t, \theta\right)$ given by:

$$\mathrm{Pr}\left(k_t = i|\widetilde{y}^*_t, \mathcal{Z}, \boldsymbol{\theta}\right) = \frac{\phi\left(h_t + \alpha_{k_t=i}, \; \sigma^2_{s=i}\right) p_{k_t=i}}{\sum_{j=1}^{10} \phi\left(\Lambda_c v_{c,t} + \Lambda_s v_{s,t} + \alpha_{k=j}, \; \sigma^2_{k_t=j}\right) p_{k_t=i}} \quad \text{for } i = 1, \cdots, 10,$$

where $\phi\left(\Lambda_c v_{c,t} + \Lambda_s v_{s,t} + \alpha_{k_t=j}, \; \sigma^2_{k_t=j}\right)$ denotes a Gaussian density evaluated at mean $\Lambda_c v_{c,t} + \Lambda_s v_{s,t} + \alpha_{k_t=i}$ and variance $\sigma^2_{k_t=i}$. Again, the values for $\alpha_{k_t=i}$ and $\sigma^2_{k_t=i}$ are given in Table 1 in Omori et al. (2007) and $v_{c,t}$ and $v_{d,t}$ denote posterior draws for the uncertainty factors (in log form).

Given $\mathrm{Pr}\left(k_t = i|\widetilde{y}^*_t, \mathcal{Z}, \boldsymbol{\theta}\right)$, posterior draws for k_t can then be generated via the inverse transform method for $t = 1, \cdots, T$ as follows:[2]

(a) Generate $\zeta_t \sim Uniform(0, \; 1)$
(b) Find the smallest $i \in \{1, 2, \cdots, 10\}$ that satisfies $\sum_{j=1}^{i} \mathrm{Pr}\left(k_t = j|\widetilde{y}^*_t, \mathcal{Z}, \boldsymbol{\theta}\right) \geq \zeta_t$
(c) Return $(k_t|\widetilde{y}^*_t, \mathcal{Z}, \boldsymbol{\theta}) = i$

---

[2]See algorithm 3.2 in Kroese et al. (2013) for a more detailed discussion of the inverse transform method for discrete random variables.

•Step 2

As discussed in Section 3.2, conditional on $\mathbf{k}$ (the data, remaining states, and parameters), we use Bayes rule to obtain the following closed-form expression for $p(\mathbf{v}|\widetilde{\mathbf{y}}^*, \mathcal{Z}_{-\mathbf{v}}, \boldsymbol{\theta})$:

$$
\mathbf{v}|\widetilde{\mathbf{y}}^*, \mathcal{Z}_{-\mathbf{v}}, \boldsymbol{\theta} \sim \mathcal{N}\left(\overline{\mathbf{d}}_v, \ \overline{\mathbf{D}}_v\right), \ \text{ where } \begin{cases} \overline{\mathbf{d}}_v = \overline{\mathbf{D}}_v \left(\boldsymbol{\Lambda}' \boldsymbol{\Sigma}_k^{-1}(\widetilde{\mathbf{y}}^* - \boldsymbol{\alpha}_k) + \mathbf{L}'_{\Phi_v} \boldsymbol{\Sigma}_v^{-1} \widetilde{\mathbf{v}}_0\right), \\ \overline{\mathbf{D}}_v = \left(\boldsymbol{\Lambda}' \boldsymbol{\Sigma}_k^{-1} \boldsymbol{\Lambda} + \mathbf{L}'_{\Phi_v} \boldsymbol{\Sigma}_v^{-1} \mathbf{L}_{\Phi_v}\right)^{-1}. \end{cases} \tag{A13}
$$

Draws from $\mathcal{N}\left(\overline{\mathbf{d}}_v, \ \overline{\mathbf{D}}_v\right)$ are obtained using the same precision sampling techniques discussed for drawing $\mathbf{f}$.

● *Initial Conditions*

We treat the vector containing the state initialization conditions (i.e., v_0) as an additional parameter to our model. We thus extend our MCMC algorithm to sample v_0. Accordingly, we rewrite (A3) as:

$$
\mathbf{L}_{\Phi_v} \mathbf{v} = \mathbf{L}_{0v} v_0 + \boldsymbol{\eta}_{\mathbf{v}} \qquad \boldsymbol{\eta}_{\mathbf{v}} \sim \mathcal{N}\left(\mathbf{0}, \ \boldsymbol{\Sigma}_{\mathbf{v}}\right), \tag{A14}
$$

where:

$$
\mathbf{L}_{0v} = \begin{bmatrix} \Phi_v \\ 0 \times I_3 \\ \vdots \\ 0 \times I_3 \end{bmatrix}.
$$

Assuming a Gaussian prior $v_0 \sim \mathcal{N}\left(\hat{\boldsymbol{\mu}}_{v_0}, \ \hat{\boldsymbol{\Sigma}}_{v_0}\right)$ and using standard regression results gives:

$$
v_0|\mathbf{y}, \mathcal{Z}, \boldsymbol{\theta} \sim \mathcal{N}\left(\overline{\mathbf{d}}_{v_0}, \ \overline{\mathbf{D}}_{v_0}\right), \ \text{ where } \begin{cases} \overline{\mathbf{d}}_{v_0} = \overline{\mathbf{D}}_{v_0} \left(\mathbf{L}'_{0v} \boldsymbol{\Sigma}_{\mathbf{v}}^{-1} \mathbf{L}_{\Phi_v} \mathbf{v} + \hat{\boldsymbol{\Sigma}}_{v_0}^{-1} \hat{\boldsymbol{\mu}}_{v_0}\right), \\ \overline{\mathbf{D}}_{v_0} = \left(\mathbf{L}'_{0v} \boldsymbol{\Sigma}_{\mathbf{v}}^{-1} \mathbf{L}_{0v} + \hat{\boldsymbol{\Sigma}}_{v_0}^{-1}\right)^{-1}. \end{cases} \tag{A15}
$$

A1.1.2 Parameter Sampling

(iv) Drawing the loadings for the IP-specific and McCracken and Ng (2016) factors

As discussed in Section 3.1, not all loadings in $\boldsymbol{\beta}$ need to sampled. Specifically, we set the usual unit-lower-triangular-matrix normalization strategy to the separately identify $\boldsymbol{\beta}_f$ from the f_t. Since f_t is 4×1 vector, we apply the above-mentioned normalization to the loadings associated with the first four industries in y_t. We reiterate that no normalization is applied to $\boldsymbol{\beta}_z$, given z_t is obtained prior to estimation via principal-component techniques and is thus treated as an "observable" within our estimation framework.

With these in mind, let $\tilde{\boldsymbol{\beta}} = \begin{bmatrix} \tilde{\boldsymbol{\beta}}_z \\ \tilde{\boldsymbol{\beta}}_f \end{bmatrix}$ denote the vector that contains only non-normalized loadings and $\odot$ be the Hadamard (or element-wise) product. We can thus recast the controls in (A1) as $\mathbf{X}\boldsymbol{\beta} = \tilde{\mathbf{w}}_f + \mathbf{Z}\tilde{\boldsymbol{\beta}}_z + \mathbf{F}\tilde{\boldsymbol{\beta}}_f$, which gives:

$$\mathbf{y} = \tilde{\mathbf{w}}_f + \mathbf{Z}\tilde{\boldsymbol{\beta}}_z + \mathbf{F}\tilde{\boldsymbol{\beta}}_f + \mathbf{L}_h \mathbf{L}_\Psi \mathbf{e}, \tag{A16}$$

where:

$$
\tilde{\mathbf{w}}_f = \left(I_T \otimes \begin{bmatrix} 1 & 0 & 0 & 0 \\ 1 & 1 & 0 & 0 \\ 1 & 1 & 1 & 0 \\ 1 & 1 & 1 & 1 \\ 0 & 0 & 0 & 0 \\ \vdots & \vdots & \vdots & \vdots \\ 0 & 0 & 0 & 0 \end{bmatrix} \right) \times \begin{bmatrix} f_1 \\ f_2 \\ \vdots \\ f_T \end{bmatrix}, \quad \mathbf{Z} = \begin{bmatrix} I_N \otimes z_1' \\ I_N \otimes z_2' \\ \vdots \\ I_N \otimes z_T' \end{bmatrix},
$$

$$
\mathbf{F} = \begin{bmatrix} (I_N \otimes f_1') \odot \left(\tilde{I}_N \otimes (1,\ 1,\ 1,\ 1) \right) \\ (I_N \otimes f_2') \odot \left(\tilde{I}_N \otimes (1,\ 1,\ 1,\ 1) \right) \\ \vdots \\ (I_N \otimes f_T') \odot \left(\tilde{I}_N \otimes (1,\ 1,\ 1,\ 1) \right) \end{bmatrix} \text{ and } \tilde{I}_N = \begin{bmatrix} 0 & 0 & \cdots & & & & 0 \\ 0 & 0 & & & & & 0 \\ \vdots & & 0 & & & & \vdots \\ & & & 0 & & & \\ & & & & 1 & & \\ & & & & & \ddots & \\ 0 & 0 & \cdots & & & & 1 \end{bmatrix}.
$$

Next, defining $\mathbf{y}_{\tilde{\beta}} = \mathbf{y} - \tilde{\mathbf{w}}_f$, $\mathbf{W} = [\mathbf{Z}\ \mathbf{F}]$, and $\mathbf{u} = \mathbf{L}_h \mathbf{L}_\Psi \mathbf{e}$, allows us to rewrite (A16) more compactly as:

$$
\mathbf{y}_{\tilde{\beta}} = \mathbf{W}\tilde{\boldsymbol{\beta}} + \mathbf{u} \quad \mathbf{u} \sim \mathcal{N}\left(0,\ \boldsymbol{\Sigma}_u\right). \tag{A17}
$$

Assuming a Gaussian prior $\tilde{\boldsymbol{\beta}} \sim \mathcal{N}\left(\hat{\boldsymbol{\mu}}_{\tilde{\beta}},\ \hat{\boldsymbol{\Sigma}}_{\tilde{\beta}}\right)$ and applying Bayes rule yields:

$$
\tilde{\boldsymbol{\beta}} | \mathbf{y}, \mathcal{Z}, \boldsymbol{\theta}_{-\tilde{\beta}} \sim \mathcal{N}\left(\overline{\mathbf{d}}_{\beta},\ \overline{\mathbf{D}}_{\beta}\right), \text{ where } \begin{cases} \overline{\mathbf{d}}_{\beta} = \overline{\mathbf{D}}_{\beta}\left(\mathbf{W}'\boldsymbol{\Sigma}_u^{-1}\mathbf{y}_{\tilde{\beta}} + \hat{\boldsymbol{\Sigma}}_{\tilde{\beta}}^{-1}\hat{\boldsymbol{\mu}}_{\tilde{\beta}}\right), \\ \overline{\mathbf{D}}_{\beta} = \left(\mathbf{W}'\boldsymbol{\Sigma}_u^{-1}\mathbf{W} + \hat{\boldsymbol{\Sigma}}_{\tilde{\beta}}^{-1}\right)^{-1}. \end{cases} \tag{A18}
$$

(v) Drawing the loadings for common and sectoral uncertainty factors

Akin to $\boldsymbol{\beta}$, we only need to draw the non-normalized loadings in $\boldsymbol{\Lambda}$. To do so, recall first from (19) in the main text that, conditional on a draw for the vector $\mathbf{k}$ (i.e., the

auxiliary state variable in the mixture-sampling approach by Omori et al. (2007)), we obtain a representation for the measurement equation that casts $\mathbf{v}$ in conditional linear Gaussian form given by:

$$\widetilde{\mathbf{y}}^* = \boldsymbol{\Lambda}\mathbf{v} + \boldsymbol{\alpha}_k + \widetilde{\mathbf{e}}_k^*. \tag{A19}$$

Next, by a change of variable we can express $\boldsymbol{\Lambda}\mathbf{v} = \tilde{\mathbf{w}}_v + \mathbf{V}\tilde{\boldsymbol{\lambda}}$, which gives:

$$\widetilde{\mathbf{y}}^* = \tilde{\mathbf{w}}_v + \mathbf{V}\tilde{\boldsymbol{\lambda}} + \boldsymbol{\alpha}_k + \widetilde{\mathbf{e}}_k^*, \tag{A20}$$

where:

$$\tilde{\mathbf{w}}_v = \left(I_T \otimes \begin{bmatrix} 1 & 1 & 0 \\ 0 & 0 & 0 \\ \vdots & \vdots & \vdots \\ 0 & 0 & 1 \\ 0 & 0 & 0 \\ \vdots & \vdots & \vdots \\ 0 & 0 & 0 \end{bmatrix} \right) \times \begin{bmatrix} v_1 \\ v_2 \\ \vdots \\ v_T \end{bmatrix}, \quad v_t = \begin{bmatrix} v_{c,t} \\ v_{d,t} \\ v_{nd,t} \end{bmatrix} \text{ for } t = 1, ..., T,$$

$$\mathbf{V} = [\mathbf{V}_c \ \mathbf{V}_s], \text{ s.t. } \mathbf{V}_c = \texttt{diag}\left(V_{c,1}, \cdots, V_{c,T}\right), \ \mathbf{V}_s = \texttt{diag}\left(V_{s,1}, \cdots, V_{s,T}\right),$$

$$V_{c,t} = v_{c,t} I_N, \quad V_{s,t} = \begin{bmatrix} 0 & 0 & \cdots & & 0 & \cdots & & 0 \\ 0 & v_{d,t} & & & 0 & \ddots & & 0 \\ \vdots & & \ddots & & \vdots & & & \vdots \\ 0 & \cdots & & v_{d,t} & 0 & \cdots & & 0 \\ 0 & \cdots & & & 0 & 0 & \cdots & 0 \\ 0 & \ddots & & & 0 & v_{nd,t} & \cdots & 0 \\ \vdots & & & & \vdots & & \ddots & 0 & \vdots \\ 0 & \cdots & & & 0 & \cdots & & 0 \\ 0 & \cdots & & & 0 & \cdots & & v_{nd,t} \end{bmatrix} \text{ and } \tilde{\boldsymbol{\lambda}} = \begin{bmatrix} \tilde{\boldsymbol{\lambda}}_c \\ \tilde{\boldsymbol{\lambda}}_d \\ \tilde{\boldsymbol{\lambda}}_{nd} \end{bmatrix}.$$

In other words, $\tilde{\mathbf{w}}_v$ collects (in stacked form) the normalization conditions; i.e., the first loading corresponding to the common, durable, and nondurable uncertainty factors is set to one, and $\tilde{\boldsymbol{\lambda}}$ denotes the $(3N-3) \times 1$ vector containing the non-normalized loadings associated with our common and sectoral uncertainty factors.

Setting $\widetilde{\mathbf{y}}_\lambda^* = \widetilde{\mathbf{y}}^* - \tilde{\mathbf{w}}_v - \boldsymbol{\alpha}_k$, assuming a Gaussian prior $\tilde{\boldsymbol{\lambda}} \sim \mathcal{N}\left(\hat{\boldsymbol{\mu}}_{\tilde{\boldsymbol{\lambda}}}, \ \hat{\boldsymbol{\Sigma}}_{\tilde{\boldsymbol{\lambda}}}\right)$ and applying Bayes rule yields:

$$\tilde{\boldsymbol{\lambda}}|\mathbf{y}, \mathcal{Z}, \mathbf{k}, \boldsymbol{\theta}_{-\tilde{\boldsymbol{\lambda}}} \sim \mathcal{N}\left(\overline{\mathbf{d}}_{\tilde{\boldsymbol{\lambda}}}, \ \overline{\mathbf{D}}_{\tilde{\boldsymbol{\lambda}}}\right), \ \text{ where } \begin{cases} \overline{\mathbf{d}}_{\tilde{\boldsymbol{\lambda}}} = \overline{\mathbf{D}}_{\tilde{\boldsymbol{\lambda}}}\left(\mathbf{V}'\boldsymbol{\Sigma}_{\mathbf{k}}^{-1}\widetilde{\mathbf{y}}_\lambda^* + \hat{\boldsymbol{\Sigma}}_{\tilde{\boldsymbol{\lambda}}}^{-1}\hat{\boldsymbol{\mu}}_{\tilde{\boldsymbol{\lambda}}}\right), \\ \overline{\mathbf{D}}_{\tilde{\boldsymbol{\lambda}}} = \left(\mathbf{V}'\boldsymbol{\Sigma}_{\mathbf{k}}^{-1}\mathbf{V} + \hat{\boldsymbol{\Sigma}}_{\tilde{\boldsymbol{\lambda}}}^{-1}\right)^{-1}. \end{cases} \quad (A21)$$

Again, the values for $\boldsymbol{\alpha}_k$ and $\boldsymbol{\Sigma}_k$ in the expression for the full conditional posterior density above are predetermined and given in Table 1 of Omori et al. (2007).

(vi) Drawing VAR coefficients for factor law of motion

We assume a VAR(1) law of motion for the vector collecting both the common and sectoral uncertainty factors (v_t) and the four IP-specific latent factors in the measurement equation (f_t). Stacking each of these over t yields:

$$\mathbf{v} = \mathbf{X}_{\mathbf{v}}\boldsymbol{\phi}_{\mathbf{v}} + \boldsymbol{\eta}_{\mathbf{v}} \qquad \boldsymbol{\eta} \sim \mathcal{N}\left(0, \ \boldsymbol{\Sigma}_{\mathbf{v}}\right), \quad (A22)$$

$$\mathbf{f} = \mathbf{X}_{\mathbf{f}}\boldsymbol{\phi}_{\mathbf{f}} + \boldsymbol{\eta}_{\mathbf{f}} \qquad \boldsymbol{\eta}_{\mathbf{f}} \sim \mathcal{N}\left(0, \ \boldsymbol{\Sigma}_{\mathbf{f}}\right), \quad (A23)$$

where:

$$
\mathbf{X_v} = \begin{bmatrix} I_3 \otimes v_0' \\ \vdots \\ I_3 \otimes v_{T-1}' \end{bmatrix} \quad \mathbf{X_f} = \begin{bmatrix} I_4 \otimes f_0' \\ \vdots \\ I_4 \otimes f_{T-1}' \end{bmatrix}.
$$

Assuming a Gaussian prior $\boldsymbol{\phi_\ell} \sim \mathcal{N}\left(\hat{\boldsymbol{\mu}}_{\phi_\ell},\ \hat{\boldsymbol{\Sigma}}_{\phi_\ell}\right)$ and applying Bayes rule yields:

$$
\boldsymbol{\phi_\ell}|\mathbf{y}, \mathcal{Z}, \boldsymbol{\theta}_{-\phi_\ell} \sim \mathcal{N}\left(\overline{\mathbf{d}}_{\phi_\ell},\ \overline{\mathbf{D}}_{\phi_\ell}\right), \ \ \text{where} \ \begin{cases} \overline{\mathbf{d}}_{\phi_\ell} = \overline{\mathbf{D}}_{\phi_\ell}\left(\mathbf{X}_\ell' \boldsymbol{\Sigma}_\ell^{-1} \boldsymbol{\ell} + \hat{\boldsymbol{\Sigma}}_{\phi_\ell}^{-1} \hat{\boldsymbol{\mu}}_{\phi_\ell}\right), \\ \overline{\mathbf{D}}_{\phi_\ell} = \left(\mathbf{X}_\ell' \boldsymbol{\Sigma}_\ell^{-1} \mathbf{X}_\ell + \hat{\boldsymbol{\Sigma}}_{\phi_\ell}^{-1}\right)^{-1} \quad \text{for } \boldsymbol{\ell} = \mathbf{v},\ \mathbf{f}. \end{cases}
$$

(A24)

(vii) **Drawing the conditional variance of first- and second-moment states**

We collect the variance parameters for the innovations driving $\mathbf{v}$ and $\mathbf{f}$ in the vectors $\boldsymbol{\sigma_v^2} = \left(\sigma_{v_c}^2,\ \sigma_{v_d}^2,\ \sigma_{v_{nd}}^2\right)'$ and $\boldsymbol{\sigma_f^2} = \left(\sigma_{f_1}^2,\ \sigma_{f_2}^2,\ \sigma_{f_3}^2,\ \sigma_{f_4}^2\right)'$. Assuming an inverse-gamma prior, $\mathcal{IG}\left(\nu,\ S\right)$, such that $S = 0.2^2(\nu-1)$, $S = (\nu-1)$ and $\nu = \frac{T}{10}$ and applying Bayes rule yields:

$$
\sigma_{v_i}^2|\mathbf{y}, \mathcal{Z}, \boldsymbol{\theta}_{-\sigma_{v_i}^2} \sim \mathcal{IG}\left(\overline{\nu}_{v_i},\ \overline{S}_{v_i}\right), \ \ \text{where} \ \begin{cases} \overline{\nu}_{v_i} = \frac{T}{2} + \nu, \\ \overline{S}_{v_i} = \frac{\sum\limits_{t=1}^{T}\left(\eta_{v_i,t}\right)^2}{2} + S \quad \text{for } i = c, d, nd \end{cases}
$$

(A25)

and

$$
\sigma_{f_i}^2|\mathbf{y}, \mathcal{Z}, \boldsymbol{\theta}_{-\sigma_{f_i}^2} \sim \mathcal{IG}\left(\overline{\nu}_{f_i},\ \overline{S}_{f_i}\right), \ \ \text{where} \ \begin{cases} \overline{\nu}_{f_i} = \frac{T}{2} + \nu, \\ \overline{S}_{f_i} = \frac{\sum\limits_{t=1}^{T}\left(\eta_{f_i,t}\right)^2}{2} + S \quad \text{for } i = 1, 2, 3, 4. \end{cases}
$$

(A26)

A1.2 Computational Performance

We assess the performance of the MCMC algorithm discussed in the previous section based on two criteria: (i) its mixing properties and (ii) computational speed.

• *Inefficiency Factors*

To address point (i), below we report two sets of inefficiency factors: one associated with the draws for the states and one associated with the draws for the parameters. Such metrics are computed using a common approach (see, e.g., Chib (2001)) given by:

$$1 + 2 \sum_{j=1}^{J} \rho_j,$$

where ρ_j is the sample autocorrelation at lag j through lag J. In our empirical application we set J to be large enough until autocorrelation tapers off. In an ideal setting where MCMC draws are virtually independent draws, inefficiency factors should be one. As a rule of thumb, inefficiency factors around twenty are typically interpreted as an indication of fast mixing.[3] Figure A1 reports boxplots to summarize inefficiency factor results. The middle line denotes the median inefficiency factor. The lower and upper lines, respectively, represent the 25 and 75 percentiles, while whiskers extend to the maximum and minimum inefficiency factors. All in all, results in Figure A1 demonstrate that our posterior sampler exhibits good mixing properties.

---

[3]Another way to interpret the inefficiency factor adopted here is to think that an inefficiency factor of 100 means that approximately 10,000 posterior draws are required to convey the same information as 100 independent draws.

Figure A1: Inefficiency Factors
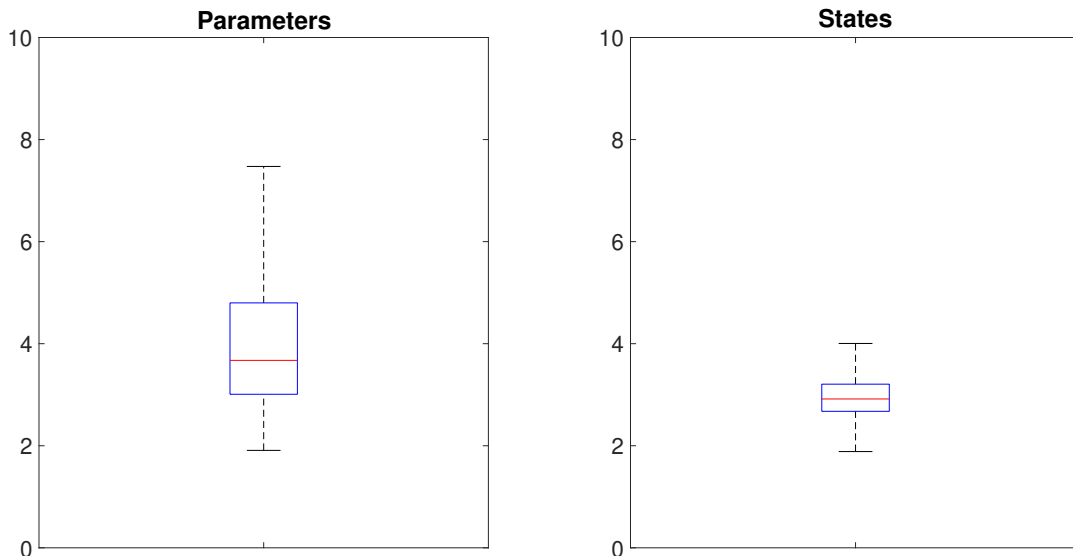
• *Computational Speed*

It takes approximately 30 minutes to generate 10,000 MCMC draws for our baseline model. Estimation routines were implemented on a desktop with an Intel Xeon E5-2690 v2 @3.00 GHz processor.

A2 Robustness Checks

In this section we report results for the robustness checks we performed. These examined the strength of our proposed measu res of common and sectoral uncertainty to (i) different parameterizations of the hierarchical common stochastic volatility model discussed in Section 2; and (ii) different VAR specifications relative to the one presented in Section 4. Overall, our findings documented in the main text carry over to all such checks.

A2.1 Uncertainty Measurement under Alternative Specifications

We begin by showing the estimated measures of common and sectoral uncertainty under different specifications of X_t in Equation (1) in the paper, i.e., the matrix collecting the

controls in the measurement equation. In particular, in addition to the baseline specification in the main text (labeled as M1 hereafter), we allowed for four alternative representations of X_t. These are summarized below in Table A1 and formalized in greater detail in Equations (A27)–(A31).

Table A1: Different Model Specifications

Model Identifier	Control Variables in X_t
M1	7 factors obtained from the FRED-MD database
	4 IP-specific factors
M2	7 factors obtained from the FRED-MD database
	4 IP-specific factors featuring stochastic volatility
M3	7 factors obtained from the FRED-MD database
M4	4 IP-specific factors
M5	4 IP-specific factors featuring stochastic volatility

$$\text{Controls for M1:} \begin{cases} X_t = [I_N \otimes z_t' \quad I_N \otimes f_t'], \\ z_t = (z_{1,t}, \cdots, z_{7,t})' \quad - \text{McCracken and Ng factors,} \\ f_t = (f_{1,t}, \cdots, f_{4,t})' \quad - \text{IP-specific factors,} \\ f_t = \Phi_f f_{t-1} + \eta_{f,t} \quad \eta_{f,t} \sim \mathcal{N}\left(0, \, \mathtt{diag}\left(\sigma_{f_1}^2, \cdots, \sigma_{f_4}^2\right)\right) \end{cases} \tag{A27}$$

$$\text{Controls for M2:} \begin{cases} X_t = [I_N \otimes z_t' \quad I_N \otimes f_t'], \\ z_t = (z_{1,t}, \cdots, z_{7,t})' \quad - \text{McCracken and Ng factors,} \\ f_t = (f_{1,t}, \cdots, f_{4,t})' \quad - \text{IP-specific factors,} \\ f_t = \Phi_f f_{t-1} + \eta_{f,t}, \quad \eta_{f,t} \sim \mathcal{N}\left(0, \, \mathtt{diag}(\exp(h_{i,t}^f))\right), \\ h_{i,t}^f = h_{i,t-1}^f + \zeta_{i,t}, \quad \zeta_{i,t} \sim \mathcal{N}\left(0, \, \sigma_{\zeta_i}^2\right) \text{ for } i = 1, ..., 4 \end{cases} \tag{A28}$$

$$\text{Controls for M3:} \begin{cases} X_t = I_N \otimes z_t', \\\\ z_t = (z_{1,t}, \cdots, z_{7,t})' \quad - \text{McCracken and Ng factors} \end{cases} \tag{A29}$$

$$\text{Controls for M4:} \begin{cases} X_t = I_N \otimes f_t', \\\\ f_t = (f_{1,t}, \cdots, f_{4,t})' \quad - \text{IP-specific factors,} \\\\ f_t = \Phi_f f_{t-1} + \eta_{f,t} \quad \eta_{f,t} \sim \mathcal{N}\left(0, \ \text{diag}\left(\sigma_{f_1}^2, \cdots, \sigma_{f_4}^2\right)\right) \end{cases} \tag{A30}$$

$$\text{Controls for M5:} \begin{cases} X_t = I_N \otimes f_t', \\\\ f_t = (f_{1,t}, \cdots, f_{4,t})' \quad - \text{IP-specific factors,} \\\\ f_t = \Phi_f f_{t-1} + \eta_{f,t}, \quad \eta_{f,t} \sim \mathcal{N}\left(0, \ \text{diag}(\exp(h_{i,t}^f))\right), \\\\ h_{i,t}^f = h_{i,t-1}^f + \zeta_{i,t}, \quad \zeta_{i,t} \sim \mathcal{N}\left(0, \ \sigma_{\zeta_i}^2\right) \ \text{for } i = 1,...,4 \end{cases} \tag{A31}$$

Figures A2 and A3 present the measures of common and sectoral uncertainty, respectively, obtained from the five variants described in Table A1. All specifications deliver similar results both qualitatively and quantitatively. Such similarity is reflected in the measures from all models being virtually perfectly correlated. We do note, however, that models M4 and M5 find higher uncertainty peaks during recessions. To select which specification suggests a more suitable fit, we conducted a model comparison based on the deviance information criteria (DIC). Details on this exercise are provided below.

Figure A2: **Common Uncertainty (Alternative Models).** Measure of uncertainty that is common across 185 industries from disaggregated Industrial Production data. Estimates denote series estimated with the baseline model M1 and alternative specifications {M2, M3, M4, M5} as described in Table A1. Vertical shaded bars correspond to NBER recession dates. $\rho_{i,j}$ for $i, j = 1, ..., 5$ and $i \neq j$ denotes the (unconditional) correlation between uncertainty measures obtained from models M_i and M_j.

Figure A3: **Sectoral Uncertainty (Alternative Models).** Measures of durables and nondurables uncertainty obtained from disaggregated Industrial Production data. Estimates denote series estimated with the baseline model M1 and alternative specifications {M2, M3, M4, M5} as described in Table A1. Vertical shaded bars correspond to NBER recession dates. $\rho_{i,j}$ for $i, j = 1, ..., 5$ and $i \neq j$ denotes the (unconditional) correlation between uncertainty measures obtained from models M_i and M_j.
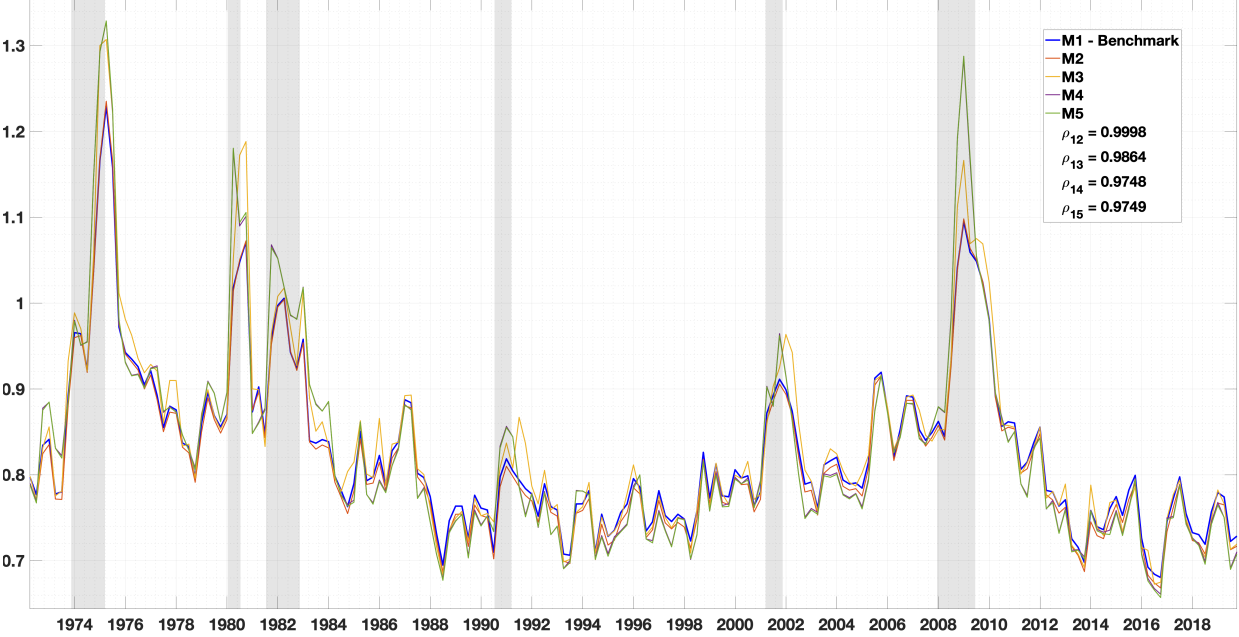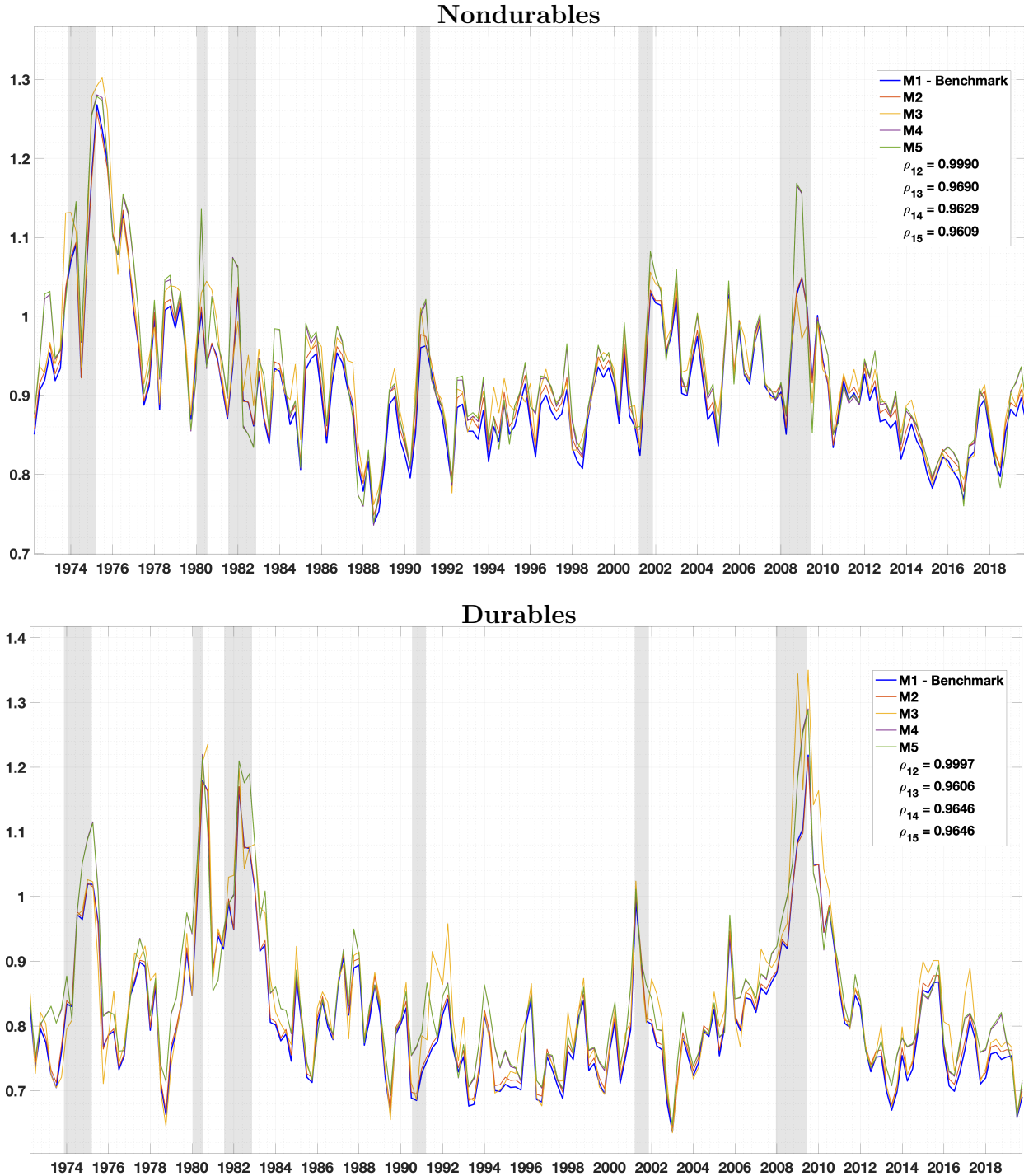
Model Comparison

Formal model comparison via Bayes-factor computation is challenging for models, such as ours, that allow for stochastic volatility. Therefore, we adopt a simpler approach to conduct model selection by computing the DIC associated with each model in Table A1. Following Berg et al. (2004) we calculate this statistic as follows:

$$\text{DIC} = -4 \sum_{l=1}^{L} \log p(\mathbf{y}|\mathcal{Z}^l_{\text{mode}}\boldsymbol{\theta}^l) + 2 \log p(\mathbf{y}|\mathcal{Z}_{\text{mode}}, \boldsymbol{\theta}_{\text{mode}}),$$

where $\mathcal{Z}_{\text{mode}}$, $\boldsymbol{\theta}_{\text{mode}}$ denotes the maximum a posteriori estimates that maximize the likelihood function, $p(\mathbf{y}|\mathcal{Z}_{\text{mode}}, \boldsymbol{\theta}_{\text{mode}})$. To compute the expression above we use $L = 50000$ post-burnin MCMC draws. Table A2 reports the DIC for each model.

Table A2: DIC Estimates

M1	M2	M3	M4	M5
$\mathbf{-9.07 \times 10^6}$	-9.06×10^6	-8.04×10^6	-8.28×10^6	-8.28×10^6

Notes: Number in bold denotes the best in-sample fit model.

A2.2 A "Strictly" Gaussian Representation

Figures A4 and A5 report our estimates for common and sectoral uncertainty based on a representation of our baseline model (M1) that excludes the scaling matrix $\mathbf{L}_\Psi$ in (A1). We refer to such a representation as the Gaussian variant of our baseline model since, as discussed in Section 2.3, the composite error term $\mathbf{L}_\Psi \mathbf{L}_h \mathbf{e}$ marginalized over $\mathbf{L}_\Psi$, follows a Student-t distribution. Uncertainty measures derived from this "strictly" Gaussian specification are in line with what we expected. In other words, we note a modest upward level shift in all uncertainty series. This follows from the fact that large volatility shifts, albeit idiosyncratic, have a greater impact on our uncertainty measures in the absence of an industry-specific scale parameter.[4]

Figure A4: **Common Uncertainty (Student-t versus Gaussian).** Measure of uncertainty common across 185 IP sectors estimated with the benchmark model M1 and its Gaussian version as an alternative modeling approach. Vertical shaded bars correspond to NBER recession dates. ρ denotes the (unconditional) correlation between the series obtained from each specification.

---
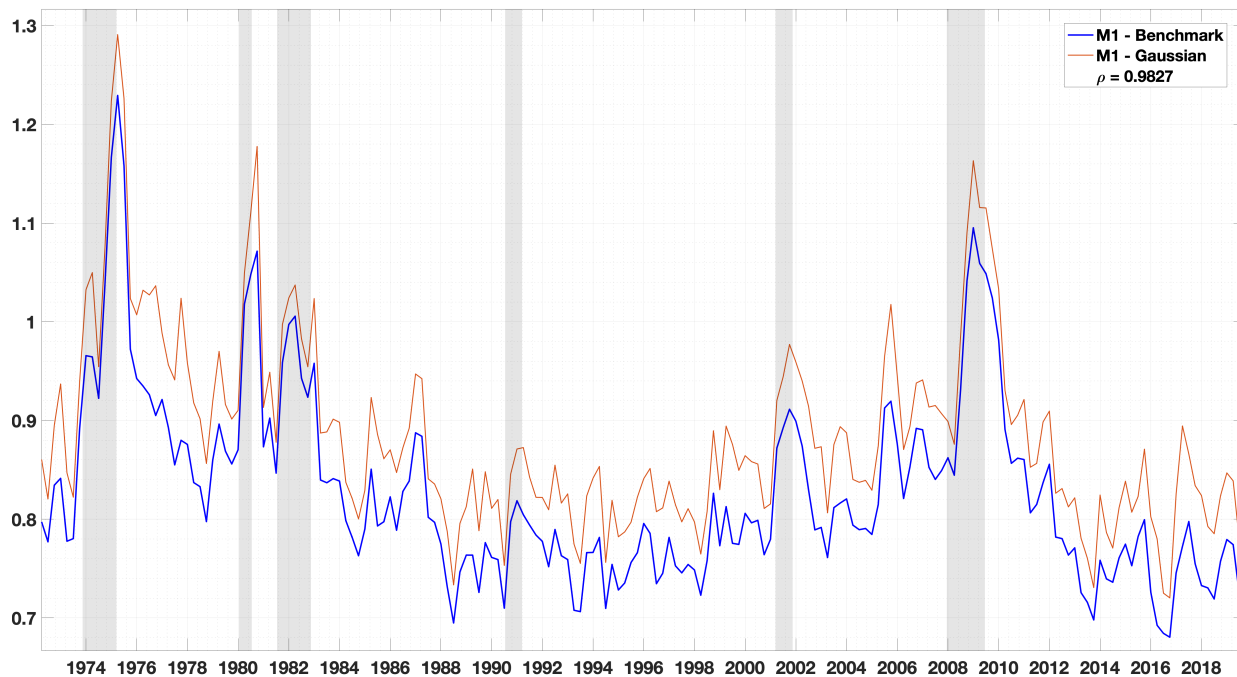
[4]We have computed the DIC for the Gaussian and Student-t versions of our baseline model, with the latter receiving considerably stronger support from the data.

Figure A5: **Sectoral Uncertainty (Student-t versus Gaussian).** Measure of nondurables and durables uncertainties estimated with the benchmark model M1 and its Gaussian version as an alternative modeling approach. Vertical shaded bars correspond to NBER recession dates. ρ denotes the (unconditional) correlation between the series obtained from each specification.
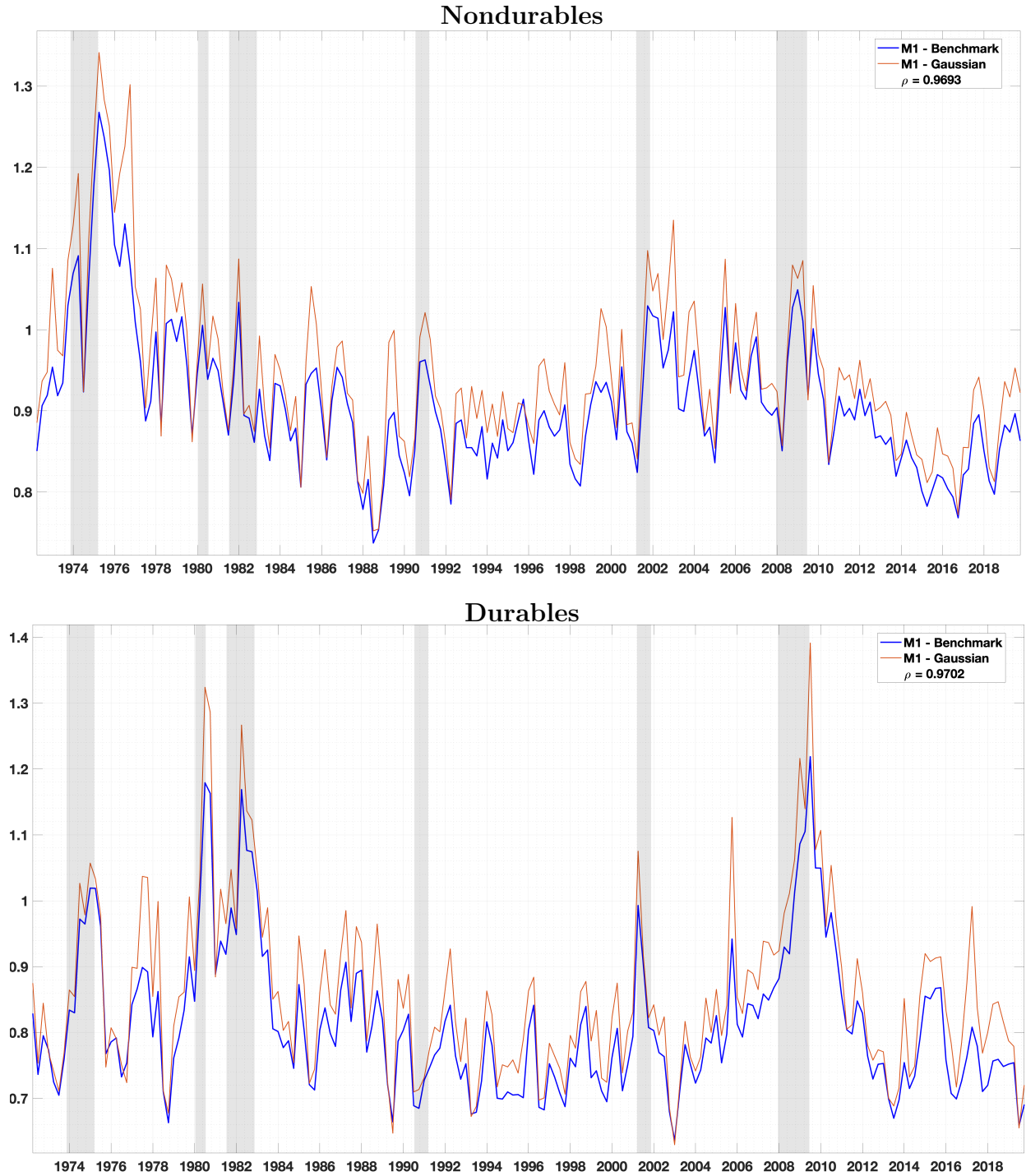
A2.3 Alternative VAR Specifications

As discussed in Section 4.5, we also examine whether our impulse response results would hold under different VAR specifications. To this end, we recompute impulse responses from VAR models with seven macroeconomic variables (similar to Bloom (2009)) and a smaller scale VAR with five macroeconomic variables (similar to Leduc and Liu (2016) and Alessandri and Mumtaz (2019)). Figures A6 and A7 present the results based on these different specifications. Notably, our key finding on the expansionary (contractionary) effect of nondurables (durables) uncertainty on economic activity carries over to all these alternative VAR specifications.

Figure A6: **Responses of Real Activity to Uncertainty Shocks (a VAR with 7 macroeconomic variables).** Impulse responses denote a one standard deviation shock to the common, nondurables, and durables uncertainty measures. In addition to the uncertainty measures, the VAR model contains $[IP, EMP, PCE, WAGE, HOURS, FFR, SP500]$ as the macroeconomic variables. Solid lines denote posterior medians, and the shaded areas represent the 67% equal-tailed posterior credible interval.

Figure A7: **Responses of Real Activity to Uncertainty Shocks (a VAR with 5 macroeconomic variables).** Impulse responses denote a one standard deviation shock to the common, nondurables, and durables uncertainty measures. In addition to the uncertainty measures, the VAR model contains $[IP, EMP, PCE, FFR]$ as the macroeconomic variables. Solid lines denote posterior medians, and the shaded areas represent the 67% equal-tailed posterior credible interval.
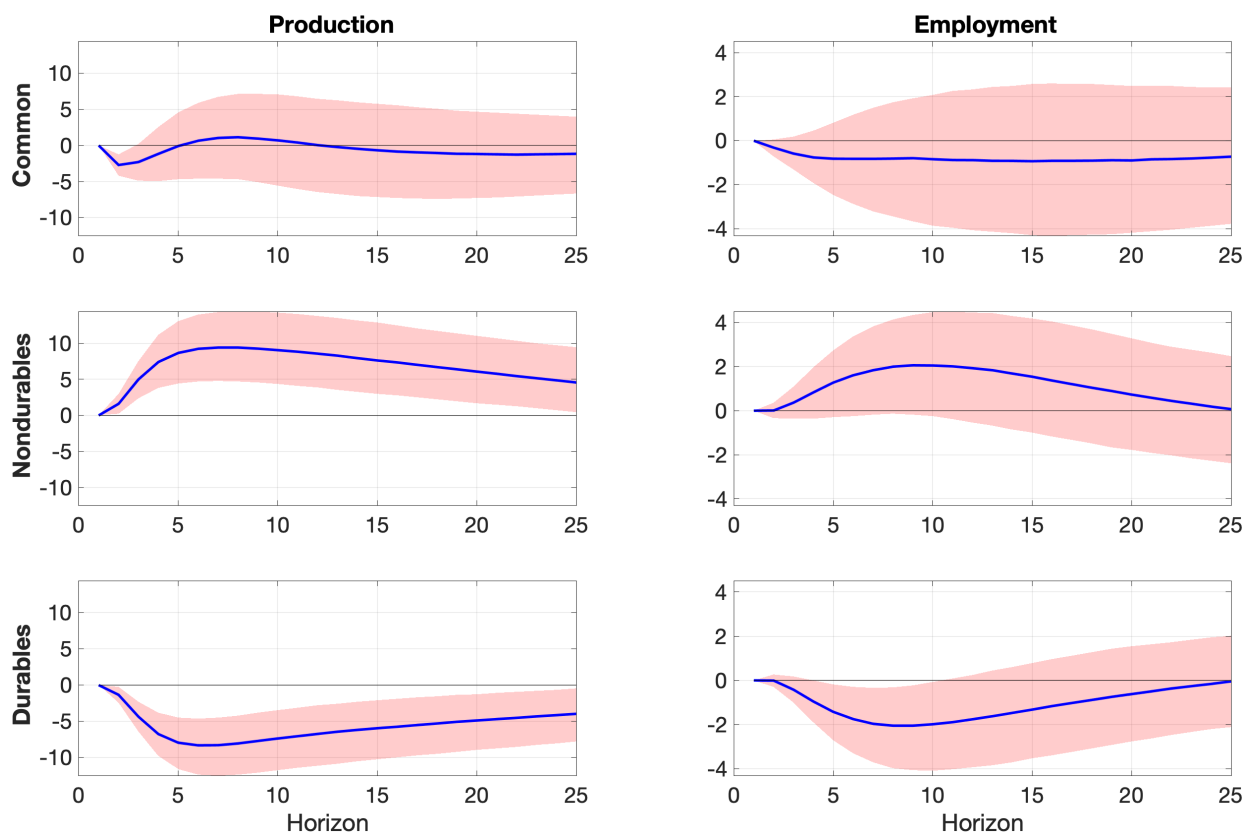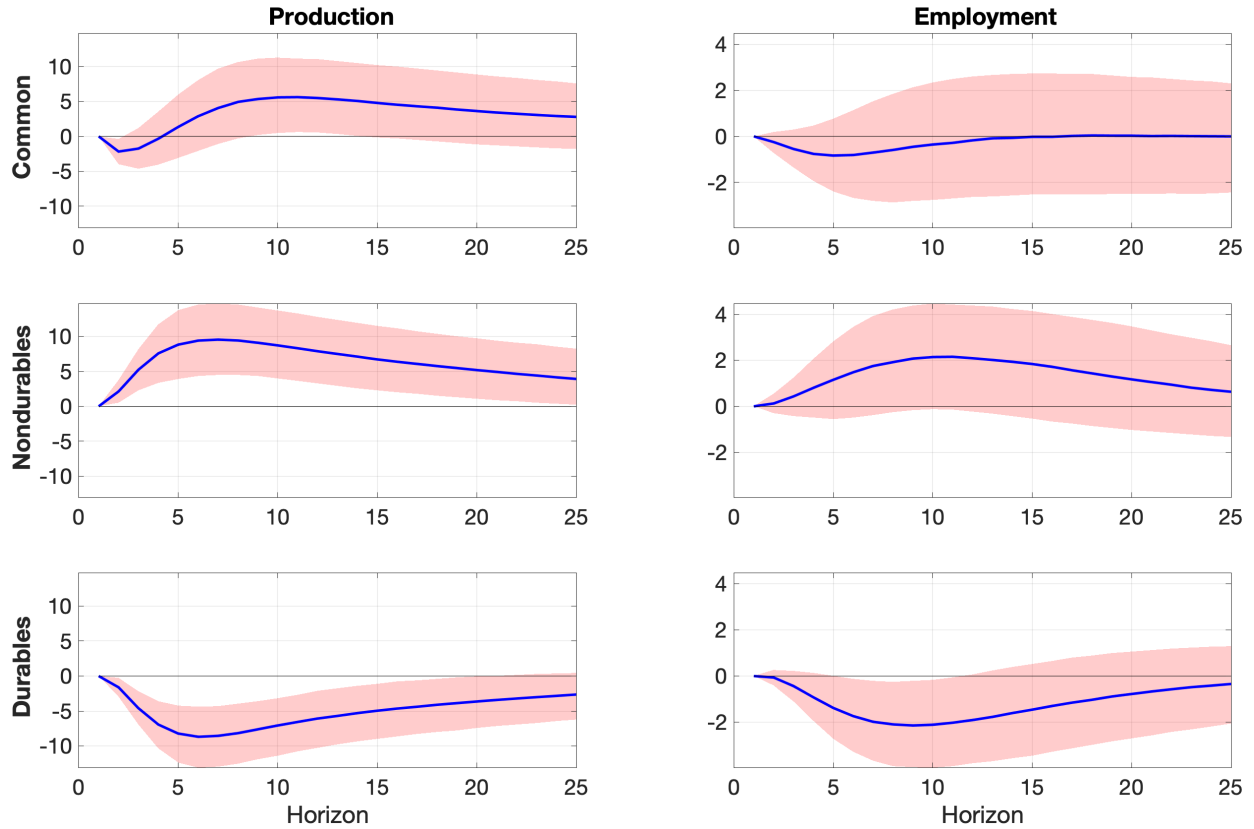
A3 Dataset Description

Table A3 provides additional details on all the industries listed in the disaggregated U.S. industrial production dataset adopted in our study. Sectors (i.e., durables and nondurables) are defined in accordance with the North American Industry Classification System (NAICS) and are thus given by the first two NAICS digits. There are 80 series in the nondurables sector, covering industries mainly in the food, textile, paper and printing, and petrochemical subsectors. The durables sector accounts for 105 series, covering industries mainly in the metal and nonmetal manufacturing, machinery and electronics, and transportation equipment subsectors.

Table A3: The table presents the U.S. Industrial Production Series with their associated sector names and NAICS codes.

Sector	Industry	NAICS Code
Manufacturing - Nondurables	Food	311
Manufacturing - Nondurables	Animal food	3111
Manufacturing - Nondurables	Grain and oilseed milling	3112
Manufacturing - Nondurables	Sugar and confectionery product	3113
Manufacturing - Nondurables	Fruit and vegetable preserving and specialty food	3114
Manufacturing - Nondurables	Dairy product	3115
Manufacturing - Nondurables	Dairy product (except frozen)	31151
Manufacturing - Nondurables	Fluid milk	311511
Manufacturing - Nondurables	Creamery butter	311512
Manufacturing - Nondurables	Cheese	311513
Manufacturing - Nondurables	Dry, condensed, and evaporated dairy product	311514
Manufacturing - Nondurables	Ice cream and frozen dessert	31152
Manufacturing - Nondurables	Animal slaughtering and processing	3116
Manufacturing - Nondurables	Animal (except poultry) slaughtering and meat processing	311611-3
Manufacturing - Nondurables	Beef	311611-3pt.
Manufacturing - Nondurables	Pork	311611-3pt.

24

Sector	Industry	NAICS Code
Manufacturing - Nondurables	Miscellaneous meats	311611-3pt.
Manufacturing - Nondurables	Poultry processing	311615
Manufacturing - Nondurables	Bakeries and tortilla	3118
Manufacturing - Nondurables	Other food	3119
Manufacturing - Nondurables	Coffee and tea	31192
Manufacturing - Nondurables	Beverage and tobacco product	312
Manufacturing - Nondurables	Beverage	3121
Manufacturing - Nondurables	Soft drink and ice	31211
Manufacturing - Nondurables	Breweries	31212
Manufacturing - Nondurables	Tobacco	3122
Manufacturing - Nondurables	Textile mills	313
Manufacturing - Nondurables	Fiber, yarn, and thread mills	3131
Manufacturing - Nondurables	Fabric mills	3132
Manufacturing - Nondurables	Textile and fabric finishing and fabric coating mills	3133
Manufacturing - Nondurables	Textile product mills	314
Manufacturing - Nondurables	Textile furnishings mills	3141
Manufacturing - Nondurables	Carpet and rug mills	31411
Manufacturing - Nondurables	Other textile product mills	3149
Manufacturing - Nondurables	Apparel	315
Manufacturing - Nondurables	Leather and allied products	316
Manufacturing - Nondurables	Paper	322
Manufacturing - Nondurables	Pulp, paper, and paperboard mills	3221
Manufacturing - Nondurables	Pulp mills	32211
Manufacturing - Nondurables	Paper mills	32212
Manufacturing - Nondurables	Paper (except newsprint) mills	322121
Manufacturing - Nondurables	Paperboard mills	32213
Manufacturing - Nondurables	Converted paper product	3222
Manufacturing - Nondurables	Paperboard container	32221
Manufacturing - Nondurables	Paper bag and coated and treated paper	32222

Sector	Industry	NAICS Code
Manufacturing - Nondurables	Other converted paper products	32223,9
Manufacturing - Nondurables	Printing and related support activities	323
Manufacturing - Nondurables	Petroleum and coal products	324
Manufacturing - Nondurables	Petroleum refineries	32411
Manufacturing - Nondurables	Aviation fuel and kerosene	32411pt.
Manufacturing - Nondurables	Distillate fuel oil	32411pt.
Manufacturing - Nondurables	Automotive gasoline	32411pt.
Manufacturing - Nondurables	Residual fuel oil	32411pt.
Manufacturing - Nondurables	Other refinery output	32411pt.
Manufacturing - Nondurables	Paving, roofing, and other petroleum and coal products	32412,9
Manufacturing - Nondurables	Chemicals	325
Manufacturing - Nondurables	Basic chemical	3251
Manufacturing - Nondurables	Organic chemicals	32511,9
Manufacturing - Nondurables	Basic inorganic chemicals	32512-8
Manufacturing - Nondurables	Industrial gas	32512
Manufacturing - Nondurables	Synthetic dye and pigment	32513
Manufacturing - Nondurables	Other basic inorganic chemical	32518
Manufacturing - Nondurables	Alkalies and chlorine	32518pt.
Manufacturing - Nondurables	Resin, synthetic rubber, and artificial and synthetic fibers and filaments	3252
Manufacturing - Nondurables	Resin and synthetic rubber	32521
Manufacturing - Nondurables	Plastics material and resin	325211
Manufacturing - Nondurables	Synthetic rubber	325212
Manufacturing - Nondurables	Artificial and synthetic fibers and filaments	32522
Manufacturing - Nondurables	Pesticide, fertilizer, and other agricultural chemical	3253
Manufacturing - Nondurables	Pharmaceutical and medicine	3254

Sector	Industry	NAICS Code
Manufacturing - Nondurables	Paints, soaps and toiletries, and other chemical products	3255-9
Manufacturing - Nondurables	Paints and other chemical products	3255,9
Manufacturing - Nondurables	Paint, coating, and adhesive	3255
Manufacturing - Nondurables	Paint and coating	32551
Manufacturing - Nondurables	Soap, cleaning compound, and toilet preparation	3256
Manufacturing - Nondurables	Plastics and rubber products	326
Manufacturing - Nondurables	Plastics products	3261
Manufacturing - Nondurables	Rubber products	3262
Manufacturing - Nondurables	Tire	32621
Manufacturing - Nondurables	Rubber products excl tires	32622,9
Manufacturing - Durables	Wood products	321
Manufacturing - Durables	Sawmills and wood preservation	3211
Manufacturing - Durables	Plywood and misc. wood products	3212,9
Manufacturing - Durables	Veneer, plywood, & engineered wood product	3212
Manufacturing - Durables	Reconstituted wood product	321219
Manufacturing - Durables	Other wood products	3219
Manufacturing - Durables	Millwork	32191
Manufacturing - Durables	Wood container and pallet	32192
Manufacturing - Durables	All other wood products	32199
Manufacturing - Durables	Manufactured home (mobile home)	321991
Manufacturing - Durables	Nonmetallic mineral products	327
Manufacturing - Durables	Clay, lime, gypsum, & miscellaneous nonmetallic mineral products	3271,4,9
Manufacturing - Durables	Clay and miscellaneous nonmetallic mineral products	3271,9
Manufacturing - Durables	Clay product and refractory	3271
Manufacturing - Durables	Pottery, ceramics, and plumbing fixture	32711
Manufacturing - Durables	Clay building material and refractories	32712

Sector	Industry	NAICS Code
Manufacturing - Durables	Other nonmetallic mineral product	3279
Manufacturing - Durables	Lime and gypsum product	3274
Manufacturing - Durables	Glass and glass product	3272
Manufacturing - Durables	Glass container	327213
Manufacturing - Durables	Cement and concrete product	3273
Manufacturing - Durables	Cement	32731
Manufacturing - Durables	Concrete and product	32732-9
Manufacturing - Durables	Primary metals	331
Manufacturing - Durables	Iron and steel products	3311,2
Manufacturing - Durables	Pig iron	3311,2pt.
Manufacturing - Durables	Raw steel	3311,2pt.
Manufacturing - Durables	Coke and products	3311,2pt.
Manufacturing - Durables	Construction steel	3311,2pt.
Manufacturing - Durables	Consumer durable steel	3311,2pt.
Manufacturing - Durables	Can and closure steel	3311,2pt.
Manufacturing - Durables	Equipment steel	3311,2pt.
Manufacturing - Durables	Miscellaneous steel	3311,2pt.
Manufacturing - Durables	Nonferrous metals	3313,4
Manufacturing - Durables	Alumina & aluminum production & processing	3313
Manufacturing - Durables	Primary aluminum production	331313pt.
Manufacturing - Durables	Secondary smelting and alloying of aluminum	331314
Manufacturing - Durables	Misc aluminum materials	331315,8pt.
Manufacturing - Durables	Aluminum extruded product	331318pt.
Manufacturing - Durables	Nonferrous metal (except aluminum) production and processing	3314
Manufacturing - Durables	Nonferrous metal (except aluminum) smelting and refining	33141
Manufacturing - Durables	Primary smelting & refining of copper	33141pt.

Sector	Industry	NAICS Code
Manufacturing - Durables	Primary smelting & refining of nonferrous metal (except copper and aluminum)	33141pt.
Manufacturing - Durables	Foundries	3315
Manufacturing - Durables	Fabricated metal products	332
Manufacturing - Durables	Forging and stamping	3321
Manufacturing - Durables	Cutlery and handtool	3322
Manufacturing - Durables	Architectural and structural metals	3323
Manufacturing - Durables	Hardware	3325
Manufacturing - Durables	Spring and wire product	3326
Manufacturing - Durables	Machine shops; turned product; and screw, nut, and bolt	3327
Manufacturing - Durables	Coating, engraving, heat treating, and allied activities	3328
Manufacturing - Durables	Other fabricated metal products	3329
Manufacturing - Durables	Ball and roller bearing	332991
Manufacturing - Durables	Machinery	333
Manufacturing - Durables	Agriculture, construction, and mining machinery	3331
Manufacturing - Durables	Agricultural implement	33311
Manufacturing - Durables	Farm machinery and equipment	333111
Manufacturing - Durables	Construction machinery	33312
Manufacturing - Durables	Mining and oil and gas field machinery	33313
Manufacturing - Durables	Industrial machinery	3332
Manufacturing - Durables	Commercial and service industry machinery and other general purpose machinery	3333,9
Manufacturing - Durables	HVAC, metalworking, and power transmission machinery	3334-6
Manufacturing - Durables	Ventilation, heating, air-con and commercial refrigeration	3334
Manufacturing - Durables	Metalworking machinery	3335

Sector	Industry	NAICS Code
Manufacturing - Durables	Engine, turbine, and power transmission equipment	3336
Manufacturing - Durables	Computer and electronic products	334
Manufacturing - Durables	Computer and peripheral equipment	3341
Manufacturing - Durables	Communications equipment	3342
Manufacturing - Durables	Audio and video equipment	3343
Manufacturing - Durables	Semiconductors & related electronic components	3344
Manufacturing - Durables	Navigational, measuring, electromedical, and control instruments	3345
Manufacturing - Durables	Electrical equipment, appliance & component	335
Manufacturing - Durables	Household appliance	3352
Manufacturing - Durables	Small electrical appliance	33521
Manufacturing - Durables	Major appliance	33522
Manufacturing - Durables	Electrical equipment except appliances	335XA
Manufacturing - Durables	Electric lighting equipment	3351
Manufacturing - Durables	Electrical equipment	3353
Manufacturing - Durables	Other electrical equipment & component	3359
Manufacturing - Durables	Battery	33591
Manufacturing - Durables	Communication & energy wire & cable	33592
Manufacturing - Durables	Other electrical equipment	33593,9
Manufacturing - Durables	Transportation equipment	336
Manufacturing - Durables	Motor vehicles	3361
Manufacturing - Durables	Automobile and light duty motor vehicle	33611
Manufacturing - Durables	Automobile	336111
Manufacturing - Durables	Light truck and utility vehicle	336112
Manufacturing - Durables	Heavy duty truck	33612
Manufacturing - Durables	Motor vehicle body and trailer	3362
Manufacturing - Durables	Truck trailer	336212
Manufacturing - Durables	Motor home	336213

Sector	Industry	NAICS Code
Manufacturing - Durables	Travel trailer and camper	336214
Manufacturing - Durables	Motor vehicle parts	3363
Manufacturing - Durables	Aerospace products and parts	3364
Manufacturing - Durables	Aircraft and parts	336411-3
Manufacturing - Durables	Railroad eqpt, ships and boats, and other transportation equipment	3365-9
Manufacturing - Durables	Railroad rolling stock	3365
Manufacturing - Durables	Ship and boat building	3366
Manufacturing - Durables	Other transportation equipment	3369
Manufacturing - Durables	Furniture and related products	337
Manufacturing - Durables	Household and institutional furniture and kitchen cabinet	3371
Manufacturing - Durables	Office and other furniture	3372,9
Manufacturing - Durables	Miscellaneous	339
Manufacturing - Durables	Medical equipment and supplies	3391

References

Alessandri, Piergiorgio and Haroon Mumtaz, "Financial regimes and uncertainty shocks," *Journal of Monetary Economics*, 2019, *101*, 31–46.

Berg, Andreas, Renate Meyer, and Jun Yu, "DIC as a model comparison criterion for stochastic volatility models," *Journal of Business and Economic Statistics*, 2004, *22*, 107–120.

Bloom, Nicholas, "The impact of uncertainty shocks," *Econometrica*, 2009, *77* (3), 623–685.

Chan, J.C.C. and I. Jeliazkov, "Efficient simulation and integrated likelihood estimation in state space models," *International Journal of Mathematical Modelling and Numerical Optimisation*, 2009, *1(1-2)*, 101–120.

Chib, Siddhartha, "Markov chain Monte Carlo methods: Computation and inference," *Handbook of Econometrics*, 2001, *5*, 3569–3649.

Kroese, Dirk P, Thomas Taimre, and Zdravko I Botev, *Handbook of Monte Carlo methods*, Vol. 706, John Wiley & Sons, 2013.

Leduc, Sylvain and Zheng Liu, "Uncertainty shocks are aggregate demand shocks," *Journal of Monetary Economics*, 2016, *82(C)*, 20–35.

McCracken, Michael W. and Serena Ng, "FRED-MD: A monthly database for macroeconomic research," *Journal of Business and Economic Statistics*, 2016, *34(4)*, 574–589.

Omori, Yasuhiro, Siddhartha Chib, Neil Shephard, and Jouchi Nakajima, "Stochastic volatility with leverage: Fast and efficient likelihood inference," *Journal of Econometrics*, 2007, *140(2)*, 425–449.